PHYSICAL LAYER AND APPLICATION LAYER ISSUES OF WIRELESS SENSOR NETWORKS

by

LINGMING WANG

Presented to the Faculty of the Graduate School of

The University of Texas at Arlington in Partial Fulfillment

of the Requirements

for the Degree of

DOCTOR OF PHILOSOPHY

THE UNIVERSITY OF TEXAS AT ARLINGTON

December 2006

To my parents.

ACKNOWLEDGEMENTS

First of all, I would like to thank my supervising professor Dr. Qilian Liang for his great support and guidance throughout the years. Back to four years ago, I was nobody but a novice to the field of wireless communication. Dr. Liang taught me from the very basics patiently, and lead me to this great area. Not only did I learn a lot from his lectures in "Wireless Communication", "Digital Communication", "Fuzzy Logic system" and "Advanced Wireless Communication", but I could also get inspirations for research from these wonderful lectures. Dr. Liang not only advises me on how to do research, but also teaches me how to be a rightful person. He has been and will be the role model for me in the rest of my life.

I am grateful to Dr. Soontorn Oraintara, Dr. Saibun Tjuatja, Dr. Zhou Wang, Dr. Jean Gao for their interest in my research and for taking time to serve in my dissertation committee.

I am also deeply indebted to current and past members of the Wireless Communications and Networking Lab, including Qinchun Ren, Haining Shu, Xinsheng Xia, Jing Liang, and Liang Zhao, for creating a stimulating research environment and making the years so enjoyable.

At last, but at most, I thank my dearest parents, Wenying Mao, Jin Wang, and my sister, Lingyan for their encouragement, sacrifice, and patience. My journey so far would not have been possible without their love and support.

November 27, 2006

ABSTRACT

PHYSICAL LAYER AND APPLICATION LAYER ISSUES OF WIRELESS SENSOR NETWORKS

Publication No. _____

Lingming Wang, Ph.D.

The University of Texas at Arlington, 2006

Supervising Professor: Qilian Liang

The potential for collaborative, robust networks of wireless sensors has attracted a great deal of research attention. For the most part, this is due to the compelling applications that wireless sensor networks will enable. Location sensing, environmental observation and surveillance, medical monitoring and a lot other applications are all gaining interest. However, wireless sensor network poses a large number of challenges. Among all, one of the most important challenges is design sensor networks that have long network lifetime, which will become especially difficult due to the energy-constrained nature of the sensor nodes. In this thesis, we focus on physical layer issues and approaches to design algorithms.

Virtual Multiple-Input Multiple-Output (MIMO) structure is very attractive to wireless sensor networks due to its huge diversity gain and potential ability to save energy. With channel state information at transmitter side, water-filling algorithm can be applied to optimize the power allocation in each sub-channel of the MIMO system based on the estimated channel matrix $\mathbf{H}$, so as to maximize the channel capacity of the system even in deep fading scenario. In reality, however, both the estimation error and the delay will

be introduced when estimate the channel. We will investigate how the estimation error will impact the optimal water-filling strategy in wireless sensor networks.

Interferences due to the hostile environment and the Multi-User Access are critical factors affecting performance of the Wireless Sensor Networks. There is clearly a need of a system that can survive from the severe interference. A hybrid Frequency Hopping/Time Hopping-Pulse Position Modulated Ultra Wide Band system is proposed for Wireless Sensor Networks to confront the hostile environment. Frequency-hopping and time-hopping are both used to get as much diversity gain as possible. An exact analysis is also derived to precisely calculate the bit error rates for both Additive White Gaussian Noise channel and path-loss channel in the presence of multitone/pulse (tone in frequency domain and pulse in time domain) interference and Multi-User Interference.

For event-centric wireless sensor networks, event detection is one of the key issues. Two methods are proposed to detect the event, one is Double Sliding Window Detection, the other one uses Fuzzy Logic approach. We evaluate the event-detection approaches based on the acoustic data collected by the test-bed in different experiments.

To further extend our work, we demonstrate that real-world sensed acoustic signals are self-similar, which means they are forecastable. We showed that a type-2 fuzzy membership function (MF), *i.e.*, a Gaussian MF with uncertain mean is appropriate to model the sensed signal strength of wireless sensors. Two fuzzy logic systems (FLS), a type-1 FLS and an interval type-2 FLS are designed to forecast signal strength. Therefore, we can not only detect the event, but also forecast the event based on the forecasted signals. Simulation results show that the interval type-2 FLS outperforms the type-1 FLS in signal strength forecasting and the performance of event detection based on the forecasted signal from type-2 FLS is much better than that based on type-1 FLS.

Another issue in wireless sensor networks is redundancy. Not only does the data of one sensor node have self-similarity, but the data from adjacent sensor nodes also have cross-similarity. Clearly, there exists highly redundancy in the collected data from sensor nodes in the neighborhood. Due to the intrinsic properties wireless sensor networks have, *e.g.*, energy constraint, bandwidth limitation, this kind of information redundancy will impact the whole networks in a negative way. We propose to use Singular-Value-QR Decomposition(SVD-QR) to reduce the redundancy in wireless sensor networks.

TABLE OF CONTENTS

ACKNOWLEDGEMENTS iii

ABSTRACT iv

LIST OF FIGURES x

LIST OF TABLES xii

Chapter

1. INTRODUCTION 1

    1.1 Wireless Sensor Networks 1

    1.2 Advantages and Applications of Wireless Sensor Network 1

    1.3 Challenges of Wireless Sensor Networks 4

    1.4 Our Strategies 7

    1.5 Thesis outline 9

2. CHANNEL CAPACITY IN MIMO WIRELESS SENSOR NETWORKS . . . 11

    2.1 Introduction 11

    2.2 Benefits of CSI at transmitter 12

    2.3 Virtual MIMO for wireless sensor networks 12

    2.4 System model 14

    2.5 One Hop Channel Capacity of MIMO Rician fading channel 17

        2.5.1 Channel Capacity with Perfect CSIT 17

        2.5.2 Optimal power allocation strategy: water-filling 17

        2.5.3 Error Model 19

        2.5.4 Channel Capacity with imperfect CSIT 20

    2.6 Numerical Results and Discussions 20

    2.7 Chapter Summary 24

3. UWB SENSOR NETWORKS IN HOSTILE ENVIRONMENT 26

3.1 Introduction . . . 26
3.2 System Models . . . 28
3.3 Multi-User Interference Analysis . . . 31
3.4 Performance Analysis with Multitone/pulse Interference . . . 34
3.5 Numerical Results and Comparisons . . . 40
3.6 Chapter Summary . . . 44
4. EVENT DETECTION IN WIRELESS SENSOR NETWORKS . . . 49
4.1 Acoustic Sensor Model . . . 50
4.2 Double Sliding Window event-detection . . . 50
4.3 Hybrid Event-Detection Based on Fuzzy Logic System . . . 52
4.3.1 Overview of Fuzzy Logic Systems . . . 52
4.3.2 Hybrid event-detection algorithm . . . 53
4.4 Simulations . . . 54
4.5 Chapter Summary . . . 55
5. EVENT FORECASTING FOR WIRELESS SENSOR NETWORKS . . . 57
5.1 Self-Similarity of Sensed Signal Strength in wireless sensor network . . . 57
5.2 Introduction Interval Type-2 Fuzzy Logic Systems . . . 58
5.2.1 Introduction to Type-2 Fuzzy Set . . . 58
5.2.2 Introduction to Type-2 FLS . . . 61
5.3 Sensed Signal Strength Forecasting Using Interval Type-2 FLS . . . 64
5.4 Event Forecasting . . . 66
5.5 Simulations . . . 67
5.6 Chapter Summary . . . 70
6. REDUNDANCY REDUCTION IN WIRELESS SENSOR NETWORKS . . . 72
6.1 Cross-similarity of Sensor Network Data . . . 72
6.2 Redundancy Reduction in Wireless Sensor Networks Using SVD-QR . . . 72
6.2.1 Introduction of SVD-QR Algorithm . . . 74
6.2.2 Examples of Redundancy Reduction Using SVD-QR . . . 76

6.3 Chapter Summary 79
7. CONCLUSION 80
7.1 Summary 80
7.2 Future directions 82
7.2.1 Multiple Event Detection in wireless sensor networks 82
7.2.2 MIMO UWB for wireless sensor networks 83
REFERENCES 84
BIOGRAPHICAL STATEMENT 96

LIST OF FIGURES

Figure		Page
1.1	Sensor nodes scattered in a sensor field	2
2.1	Virtual MIMO architecture in WSN	13
2.2	Average Channel Capacity for 3×3 MIMO with Rician fading	21
2.3	Average Channel Capacity for 3×3 MIMO with Rayleigh fading	22
2.4	Average Channel Capacity for 6×6 MIMO with Rician fading	22
2.5	Average Channel Capacity for 6×6 MIMO with Rayleigh fading	23
2.6	Average Channel Capacities for 6×6 and 3×3 MIMO systems	24
2.7	Average Channel Capacities for 3×6 and 6×3 MIMO systems	24
3.1	An example of the waveform of a 2-PPM signal	35
3.2	The MAP detection rule for all the cases	37
3.3	The average SER for different N_s	41
3.4	The average BER for different N_S	42
3.5	The average SER for different E_b/P_J	43
3.6	The average BER for different E_b/P_J	44
3.7	The average SER for different q	45
3.8	The average BER for different q	45
3.9	The average BER for different N_F	46
3.10	The average SER for different N_u	46
3.11	The average BER for different N_u	47
3.12	The average SER for different λ	47
3.13	The average BER for different λ	48
4.1	The response of the double sliding window event-detection algorithm	51
4.2	The structure of a fuzzy logic system	53

4.3 MFs used to represent the linguistic labels 54
4.4 240 sensed data set, the sample period is 1024ms 55
5.1 The deployment of eight sensor nodes in our experiments 59
5.2 The *variance-time* plot (fixed source) 59
5.3 The *variance-time* plot 59
5.4 Representation of a Gaussian type-2 set 64
5.5 The interval type-2 MFs with fixed std and uncertain mean 65
5.6 The structure of a type-2 FLS 65
5.7 Sensed data for 1024 seconds. (The sample period is 1024ms) 71
5.8 The forecasting RMSE by two FLSs 71
6.1 The *variance-time* plot for mixed sensor data 73

LIST OF TABLES

Table		Page
3.1	Parameters of the example FH/TH-PPM UWB system	40
4.1	Rules for event-detection. Antecedent 1 is E_s, Antecedent 2 is m_n.	55
4.2	Probabilities of detection and false alarms	56
5.1	The parameters in type-1 and interval type-2 FLSs	68
5.2	Initial values of the parameters in type-1 and interval type-2 FLSs	68
5.3	Average absolute error between the forecasted and actual time stamp . .	70

CHAPTER 1

INTRODUCTION

1.1 Wireless Sensor Networks

The infusion and maturation of the micro-electro-mechanical systems (MEMS), wireless communications, and digital electronics technologies have advanced the development of low-cost, low-power, multi-functional sensor nodes, which are generally small size and can communicate untethered in short distance. Theses sensor nodes are typically equipped with processor & memory (together as the processing unit), power unit(usually battery), wireless communication interfaces and various sensors, which can perform sensing, data processing, and communication respectively. Usually a large number of these tiny, not expensive sensor nodes will work collaboratively so as to collect the useful and accurate information from their surrounding areas and deliver to the base stations.

The position of sensor nodes and the communication topology can either be carefully engineered (e.g., placed one by one by a human or a robot) or be totally random(e.g., dropped by a plane, throwing by a catapult). The latter is more attractive to potential users, because it makes the access to uninhabited terrains and disaster relief operations feasible. On the other hand, due to the lack of *a priori* infrastructure support in this random deployment environments, the sensor nodes must self-organize into networks, referred to as *Wireless sensor networks* (WSN).

1.2 Advantages and Applications of Wireless Sensor Network

The sensor nodes are usually scattered in a sensor field as shown in Figure 1.1. These sensor nodes may equipped with a lot of different types of sensors such as seismic, mag-

netic, thermal, visual, infrared, acoustic, and radar, which make Wireless Sensor Network be able to monitor various ambient conditions that include temperature, humidity, vehicular movement,lightning condition, pressure, soil makeup, noise levels, the presence or absence of certain objects, mechanical stress levels on attached objects, the current characteristics such as speed, direction, and size of an object [21].

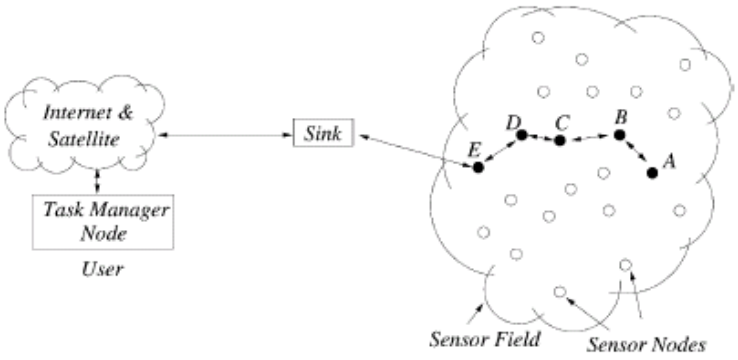

Figure 1.1. Sensor nodes scattered in a sensor field.

Besides the various sensing ability, the other strong points of Wireless Sensor Networks can be concluded as [2]:

- Ensuring greater signal to noise ratio (SNR) by combining information from sources with different spatial perspectives.

- Allowing greater fault tolerance through a high level of redundancy. [56]

- Providing coverage of a large area through the union of the individual nodes coverage area.

- Improving sensing performance by including multiple sensors.

- Overcoming environmental effects by having sensors at close proximity to the object of interest.

- Localizing discrete phenomenon through each sensor's limited range and combining information with other sensor nodes.

- Deployed in regions where infrastructure for replenishing energy/power is not available.

The advantages of Wireless Sensor Network make it have a wide range of potential applications, which can be categorized into military, environment, health, home and other commercial areas:

- *Military* applications include battlefield surveillance; monitoring friendly forces, equipment and ammunition; reconnaissance of opposing for and terrain; battle damage assessment; nuclear, biological and chemical attack detection and reconnaissance; and object targeting and tracking [3, 55].

- *Environmental* applications include forest fire detection [12]; bio-complexity mapping of the environment [11, 30]; flood detection [10](ALERT system [5]); and precision agriculture.

- *Health* applications include tele-monitoring of human physiological data [49, 50, 66]; tracking and monitoring doctors and patients inside hospitals; and drug administration in hospitals [80].

- *Home* applications include home automation [69]; human-centered or technology-centered smart environment [1, 20, 34], detecting and monitoring car thefts.

The number of sensor nodes deployed in studying a phenomenon may be in the order of hundreds or thousands. Some applications may require the number of sensor nodes reach an extreme value of millions. As a result, the cost of a single sensor node should be kept as low as possible to justify the overall cost of the networks. In [71], it is claimed that the cost of a sensor node should be much less 1$ in order for the sensor network to be feasible.

1.3 Challenges of Wireless Sensor Networks

There are several thrust area in the operations of the wireless sensor networks:

- *Energy Constraint*

  As a micro-electronic device, sensor node can be equipped with a limited power source, i.e., $< 0.5Ah, 1.2V$. Besides, most of the Wireless Sensor Networks are set remotely, it is impossible to replenish the power source. Therefore, sensor node lifetime shows a strong dependence on battery lifetime. The dead of few nodes will cause significant changes of the topology, and directly influence the lifetime of the network [43]. On the other hand, in some scenario, Wireless Sensor Networks are expected to keep functioning for years to decades. Hence, energy conservation and power management take on additional importance in the design of Wireless Sensor Networks.

  The basic task of sensor nodes is to detect events, perform simple local data processing, and transmit the data. Energy consumption can hence be divided into three domains:

  - Sensing;
  - Data processing, including AD/DA and digital signal processing;
  - Communication.

  According to [89], the sensing and signal processing parts operate at low frequency and consume less than $1mW$. This is over an order of magnitude less than the energy consumption of the communication part, which involved both data transmission and reception. Mixers, frequency synthesizers, voltage control oscillators, phase locked loops (PLL) and power amplifiers, all consume valuable power in the transceiver circuitry. The example in [70] effectively illustrates this property. Assuming Rayleigh fading channel, and the pass loss exponential parameter is 4, the energy cost of transmitting $1KB$ data of a distance of $100m$ is approximately the same as that for executing 3 million instructions by a 100 MIPS (million instructions per second) processor. Therefore, less communication/data exchange between sensor nodes but more local processing implemented by single sensor node is more attractive in terms of the energy consumption and prolonging the lifetime of the Wireless Sensor Networks.

- *Unreliable communication*

  Depending on the applications, Wireless Sensor Networks are set up either very close to or directly inside the phenomenon to be observed. Therefore, sensor nodes usually work unattended in remote geographic areas, for example:
  - in a battle field beyond the enemy lines;
  - in the bottom of an ocean;
  - on the surface of an ocean during a tornado;
  - attached to fast moving vehicles.

  Under such harsh condition, sensor nodes may suffer potential failure due to the unreliability of the sensor nodes, high channel bit error ratio, intentional jamming

and interference, multi-path fading. All of these make the communication highly unreliable.

- *Fault Tolerance and Redundancy Reduction*

  Some sensor nodes may fail or be blocked because of the energy outage, physical damage, or environmental interference. The failure of sensor nodes should not affect the overall task of the sensor network. For example, if sensor nodes are being deployed in a battlefield for surveillance and detection, the sensed data are very critical, meanwhile, sensor nodes can be destroyed by the hostile action. The high unpredictable nature of Wireless Sensor Networks necessitates a high redundancy to guarantee fault tolerance, which refers the ability to sustain sensor network functionalities without any interruption due to sensor node failure [37, 64, 77]. On the other hand, Wireless Sensor Networks face the problem of energy constraint, and the limited memory, storage, bandwidth. Hence, how to optimize the resources, and reduce the redundancy without decreasing the performance is another issue need to be paid attention to.

- *Quality of Service*

  For the traditional communication system, we use *Bit Error Rate* (BER) and *channel capacity* to evaluate the physical layer performance of system. However, the missions of Wireless Sensor Networks are not only to transmit the information accurately, but also to observe and monitor the physical world. Therefore, event detection becomes another important assignment of Wireless Sensor Networks. Obviously, when we evaluate the quality of service (QoS) of Wireless Sensor Networks, the probability of detection (P_d), the probability of false alarm (P_{fa}) should also be included.

1.4 Our Strategies

The architecture of the wireless sensor networks can be layered as: *application layer*, *transport layer*, *network layer*, *data link layer*, *physical layer* [3]. Different applications can be carried on and used on the application layer depending on the tasks. The transport layer helps to maintain the flow of data if the sensor networks application requires it [70, 72]. This layer is especially needed when the system is planned to be accessed through Internet or other external networks [3]. The network layer takes care of routing the data supplied by the transport layer. A lot of network layer protocols have been proposed for wireless sensor networks, e.g., LEACH [33], SPIN [32], directed diffusion [39], GPER [102], energy efficient routing protocols [51]. The data link layer is responsible for the multiplexing of data streams, data frame detection, medium access and error control, e.g., energy efficient scheduling for wireless sensor networks [104], energy efficient clustering for wireless sensor networks [105]. The physical layer addresses the needs of simple and robust modulation, transmission and receiving techniques. The underlying physical layer can be exploited by both system-level and node-level algorithms to achieve *energy-efficient* and *QoS* satisfied solutions in wireless sensor networks.

In this dissertation, we presented physical layer and application layer driven approaches to algorithm design for wireless sensor networks, including:

- *MIMO wireless sensor networks.*

  Virtual multiple-input multiple-output (MIMO) communication architecture has recently been applied in energy-constraint, distributed wireless sensor networks so as to economize energy consumption through its potential huge diversity gain [17, 47, 48]. With channel state information (CSI) at transmitter, we can design algorithms (e.g., water-filling algorithm) to be applied to optimize the power allocation in each sub-channel of the MIMO system based on the already known channel matrix $\mathbf{H}$, so as to maximize the channel capacity of the system even in the deep fading

scenario. However, in reality, the CSI at the transmitter may not be accurate due to either the estimation error, or the time delay. We will investigate how the error impact the channel capacity under this circumstance.

- *Ultra WideBand sensor networks.*

  Since 2002 there has been great increasing popularity of commercial applications based on Ultra Wide Band (UWB) communication techniques. UWB systems have potentially low complexity and low cost; have a very good time domain resolution, which facilitates location and tracking applications. This has ignited the interest in the use of this technology for wireless sensor networks. A UWB based sensor network is proposed in [87] for civil infrastructure health monitoring.

  We proposed a hybrid Frequency Hopping/Time Hopping-Pulse Position Modulated (FH/TH-PPM) Ultra Wide Band system for wireless sensor networks, where frequency hopping and time hopping are both used to get as much diversity gain as possible. However, neither multi-user interference or hostile interference in Ultra Wide Band sensor networks can be neglected. We first derived theoretical performance formula when the low duty-cycle in Ultra Wide Band system and the large number of sensor nodes in a wireless sensor networks are considered, and then focused our study on the theoretical analysis of the physical layer performance in the presence of multitone/pulse (tone in frequency domain and pulse in time domain) interference and Multi-User Interference.

- *Event-centric wireless sensor networks.*

  The main goal of wireless sensor networks is to sense the physical world, collect the data, and then send back to the users. Usually, people are more interested in unexpected data. For example, in a scenario of battlefield, people are more interested in the appearance of enemies. If a wireless sensor network is set up to monitor forest-fire, the unusual increasing of the temperature should be a necessary

warning to people. Both the appearance of enemies and the unusual increasing of the temperature can be seen as *events*. Because of the energy constraint of wireless sensor networks mentioned previously, the ideal state of wireless sensor networks should be event-driven, so that the communication component, which cost the most of the energy, can be powered off most of the time. Only when certain sensor nodes detect an event, the radio-frequency channel will be triggered, and transmit the useful information out. Our approach is based on no other than the *event-driven* characteristic that wireless sensor networks have so as to reserve energy and prolong the lifetime of the networks. A node-level power-mode scheduling algorithm [79] will be used to save energy by managing the active and sleep modes of the underlying device. Risk that might miss the event will be introduced if we cannot schedule the modes very well. Hence, to detect and predict events accurately becomes a crucial issue.

- *Redundancy reduction in wireless sensor networks*.

  Redundancy among neighborly nodes is one of the properties of wireless sensor network. It can guarantee fault-tolerance, on the other hand, it leads to the cost of energy, bandwidth, memory, and the occurrence of interference. Therefore, we propose to let one or two nodes to represent the whole neighboring group, let the others be at the idle state to save the energy of themselves, and meanwhile prolong the life-time of the whole network. To reduce the number of the working nodes can also save the bandwidth of the network and reduce the multi-user interference and probability of collision.

1.5 Thesis outline

This thesis consists of 4 main chapters. Chapter 1 is this introduction. The remaining chapters follow the contributions outlines above. A brief outline of each chapter is as

follows.

Chapter 2 discusses how the estimation error and time delay of the channel state information at the transmitter side will impact the channel capacity of a MIMO sensor network system.

Chapter 3 proposes a hybrid Frequency Hopping/Time Hopping-Pulse Position Modulated (FH/TH-PPM) Ultra Wide Band system for wireless sensor networks, which is targeting in hostile environment applications. It then focuses on the interference and performance analysis in such circumstances.

Chapter 4 proposes two event-detection approaches in wireless sensor networks, including double sliding scheme and hybrid approach based on Fuzzy Logic System.

Chapter 5 shows an energy-efficient event-centric wireless sensor network. Then it shows how to use type-2 Fuzzy logic system to forecast the sensed signal and the event.

Chapter 6 studies redundancy problem in wireless sensor networks. It proposes to use SVD-QR to select the principal data sets from particular sensor nodes to represent the all the sensor nodes in the neighborhood effectively.

The last chapter provides the conclusion. This chapter summarizes the main result of the thesis, and outlines future research directions.

CHAPTER 2

CHANNEL CAPACITY IN MIMO WIRELESS SENSOR NETWORKS

2.1 Introduction

During the last decade, wireless communication has occurred tremendous growth in data, voice, and video appliances. Cell phones and laptops with wireless capability are becoming common. The data rate of wireless Local Area Networks (LAN) has reached unprecedented levels of hundreds of megabits per seconds [65, 40], allowing seamless connectivity.

One of the techniques to enable such advances, and a breakthrough in wireless communications, is the adoption of multiple antennas at both the transmitter and the receiver. Multiple-input multiple-output (MIMO) systems allow a growth in transmission rate linear in the minimum of the numbers of antennas at each end [84]. They also enhance link reliability and improve coverage [68]. MIMO technology is now entering next generation cellular and wireless LAN products [40, 41, 42], with the promise of widespread applications in the near future.

The remainder of this chapter is organized as follows. In section 2.2 the benefit of the CSI at transmitter side will be introduced. We briefly present the relay virtual MIMO architecture for wireless sensor networks in section 2.3, and the underlying one-hop MIMO system model will be presented in 2.5. Whereafter, we investigate the channel capacity with imperfect CSI in section**??**. The numerical results will be presented in section2.6.

2.2 Benefits of CSI at transmitter

A wireless channel exhibits time, frequency, and space selective variations, known as fading, which arises due to Doppler, delay, and angle spreads in the scattering environment [44, 73]. We focuses on the time-varying channel, assuming frequency-flat and negligible angle spread.

The theoretical capacity gain of MIMO channels is tremendous, however, it depends heavily on how accurately we know the channel. Specifically, when the instantaneous channel gains, i.e., channel state information (CSI), are known perfectly at the transmitter of the MIMO system, the transmitter can adapt its transmission strategy relative to the instantaneous channel state, so the maximum MIMO channel capacity can be achieved.

In a frequency-flat MIMO system, channel information can be two dimensional: temporal and spatial. Temporal CSI at transmitter (CSIT) - channel information across multiple time instances - provides negligible capacity gain at medium-to-high SNRs [25]. Spatial CSIT, which is channel information across antennas, on the other hand, offers potentially significant increase in channel capacity at all SNRs. For example, in a 4-transmit 2-receiver antenna system, transmit channel knowledge can more than double the capacity at -5dB SNR and add 1.5bps/Hz to the capacity at 5dB SNR [88].

2.3 Virtual MIMO for wireless sensor networks

Recently, virtual MIMO architecture has also been applied in energy-constraint, distributed wireless sensor networks so as to economize energy consumption [17, 47, 48]. In these implementations, the underlying MIMO concepts include the simple Alamouti scheme [4] and the virtual Bell Labs Layered Space-time (V-BLAST) architecture [101].

We will first briefly review the virtual MIMO architecture applied in wireless sensor networks.

The nodes in a wireless sensor networks are usually of small dimensions. Thus it may not be realistic to assume these inexpensive sensor nodes are equipped with multiple antennas. [17] first proposed to realize MIMO communication architecture in a wireless sensor network consisting of single-antenna sensor nodes via sensor cooperation. The MIMO architecture applied here is shown in Fig. 2.1

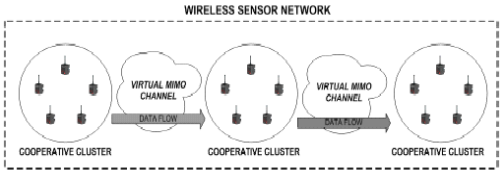

Figure 2.1. Virtual MIMO architecture in WSN.

There is a transmitter cluster, which is composed of a group of N_T cooperative sensor nodes, communicating with a receiver cluster, which is compose of a set of N_R cooperative sensor nodes. In order to fulfil the communication, the transmitter cluster should do:

- broadcasting the data within the cluster, so that all the active sensor nodes inside the cluster can encode and send out the data during the MIMO transmission;

- transmitting the data via the $N_T * N_R$ MIMO channel.

These two functionalities should be carried out in two orthogonal channel. Here, we assume time division (TD) scheme is applied. These two TD channels are referred as *Intra-cluster* channel and *Inter-cluster* channel respectively. For *Intra-cluster* channel, it is falling into the broadcast capacity region. In the *Inter-cluster*, the N_T sensor nodes

jointly transmit data to the receiver cluster by using a $N_T * N_R$ virtual MIMO channel. Hence, we will mainly focus on the *Inter-cluster* MIMO channel.

Channel capacity for MIMO channel has been intensively studied in different scenarios since the pioneer work by Winters [100] and Telatar [84]. Most of them modeled the channel as fully scattering, *i.e.*, Rayleigh fading channel. The Rayleigh fading model is a reasonable assumption for many fading environments encountered in practical communication systems. However in some other cases, (*e.g.*, in Wireless LAN application, and for sure, wireless sensor networks fit in this scope), there exists a strong deterministic Line-Of-Sight (LOS) component between the transmitter and receiver, which gives rise to Rician fading model. The Rician distribution is characterized by the Rice factor, k, which reflects the relative strength of the direct LOS path component. When $k = 0$, this model reduces to Rayleigh fading and $k \to \infty$ the model reduces to AWGN channel. The capacity of a Rician channel with receiver CSI but without any knowledge even the Rice factor at the transmitter has been studied in [22, 18]. [46] assumes that there is perfect CSI at receiver (CSIR), meanwhile the transmitter has partial CSI, *i.e.*, the knowledge of the value of the Rice factor.

In this thesis, we assume that the transmitter has full/partial CSI, but with estimation error and time delay. We will investigate how the error and delay impact the channel capacity.

2.4 System model

We consider N_T transmit sensor nodes and N_R receive sensor nodes which equal to N_T transmit antenna and N_R receive antenna respectively. Throughout, we assume that $N_R \geq N_T$. The discrete-time received signal in such a system can be modeled in matrix

form as

$$\mathbf{y}(i) = \mathbf{H}(i)\mathbf{x}(i) + \eta(i) \tag{2.1}$$

where at symbol time i, $\mathbf{x}(i)$ is the $N_T \times 1$ vector of transmitted signal on the N_T transmitting sensor nodes, $\mathbf{y}(i)$ is the $N_R \times 1$ vector of received signal on the N_R receiving sensor nodes, and $\eta(i)$ is the $N_R \times 1$ additive receiver noise vector. We assume the components of the noise $\eta(i)$ to be independent, zero-mean, circularly symmetric complex Gaussian with independent real and imaginary parts having equal variances. The noise is also assumed to be independent with respect to the time index, and

$$R_\eta = E[\eta(i)\eta(i)^H] = \sigma_\eta^2 I_{N_R}, \tag{2.2}$$

where $I_{N_R} \in \mathbb{C}^{N_R \times N_R}$ denotes the identity matrix, and A^H denotes the hermitian conjugate of the matrix A.

The Channel State Information (CSI) is defined as the channel matrix $\mathbf{H}(i) \in \mathbb{C}^{N_R \times N_T}$. The (m, n)-th element of the matrix $\mathbf{H}(i)$ represents the fading coefficient value at time i between the m-th receiving sensor node to the n-th transmitting sensor node. The $\mathbf{H}(i)$ corresponding to each channel realization is assumed to be independent from that of other realizations, *i.e.*, $\mathbf{H}(i)$ and $\mathbf{H}(j)$ are independent when $i \neq j$. In this sense, the time index i can be dropped so as to simplify notation.

In Rician fading the elements of $\mathbf{H}$ are nonzero mean, complex Gaussian variables. Hence, we can model the channel matrix $\mathbf{H}$ as a sum of two components, a fixed (LOS) compo-

nent and a variable (or scattered) component,

$$\mathbf{H} = \overline{\mathbf{H}} + \widetilde{\mathbf{H}} \tag{2.3}$$

and

$$\begin{aligned} \overline{\mathbf{H}} &= E\{\mathbf{H}\} \\ &= \frac{\mu}{\sqrt{2}}(1+j)\Psi_{N_R,N_T} \end{aligned} \tag{2.4}$$

where $j = \sqrt{-1}$, Ψ_{N_R,N_T} is defined as the $N_R \times N_T$ matrix of all ones. $E\{\cdot\}$ is an expectation operation. $\widetilde{\mathbf{H}}$ is a complex distributed matrix with zero-mean, denoted as $\widetilde{\mathbf{H}} \sim \mathcal{N}_c(\mathbf{0}, \mathbf{I}_{N_T} \bigotimes \mathbf{\Sigma})$, with the probability density function (pdf) [15, 45]

$$f_{\widetilde{H}}(\widetilde{\mathbf{H}}) = \frac{1}{(\pi)^{N_T N_R}|\Sigma|^{N_T}} e^{-tr[\Sigma^{-1}\widetilde{H}\widetilde{H}^H]}, \tag{2.5}$$

where tr denotes the trace of a matrix, Σ is the Hermitian covariance matrix of the columns (assumed to be the same for all the columns) of $\widetilde{\mathbf{H}}$,

$$\Sigma = 2\ \sigma^2\ \mathbf{I}_{N_R}. \tag{2.6}$$

The strength of the LOS component can be indicated by the *Rician K* factor,

$$K = 10\ log_{10}(\frac{|\mu|^2}{2\sigma^2})\ dB. \tag{2.7}$$

In the case of Rayleigh fading, which is an extreme scenario of Rician fading, $K = 0$. The parameters should be normalized as

$$|\mu|^2 + 2\,\sigma^2 = 1, \tag{2.8}$$

so that the signal-to-noise ratio (SNR) will not be scaled by the channel. We also assume that the channel is block fading [8], *i.e.*, $\mathbf{H}$ remains constant over $T \geq N_T$ symbol periods and changes in an independent fashion from block to block.

2.5 One Hop Channel Capacity of MIMO Rician fading channel

The CSI is the channel matrix $\mathbf{H}$. Based on different knowledge of the CSI, we can get different system performances, and channel capacities.

2.5.1 Channel Capacity with Perfect CSIT

If CSIT is available, the transmitting sensor nodes can adapt its transmission strategy according to this CSI. The channel capacity of such a MIMO system with perfect CSIT is nothing but the average of the capacities achieved with each channel realization. The formula is given in [24]

$$C = \mathbb{E}_{\mathbf{H}}[\max_{Q:tr(Q)=P} \log|\mathbf{I}_{\mathbf{N_R}} + \mathbf{HQH^H}|] \tag{2.9}$$

where $\mathbf{Q}$ is the input covariance matrix as

$$\mathbf{Q} = E(\mathbf{xx^H}). \tag{2.10}$$

2.5.2 Optimal power allocation strategy: water-filling

With CSI at both the receiver and the transmitter, optimal power allocation strategy based on the $\mathbf{H}$ should be applied to maximize the channel capacity in (2.9) [85]. The joint singular value decomposition (SVD) and *water-filling* power allocation technique provides the optimum solution [78].

The SVD of the channel matrix $\mathbf{H}$ is presented as

$$\mathbf{H} = \mathbf{U}\ \mathbf{\Lambda}\ \mathbf{V}^H \tag{2.11}$$

where $\mathbf{U} \in \mathbb{C}^{N_R \times N_R}$ is an unitary matrix of orthonormalized eigenvector of $\mathbf{H}\mathbf{H}^T$, $\mathbf{V} \in \mathbb{C}^{N_T \times N_T}$ is an unitary matrix of orthonormalized eigenvector of $\mathbf{H}^T\mathbf{H}$, and $\mathbf{\Lambda} \in \mathbb{C}^{N_R \times N_T}$ is a rectangular matrix whose diagonal elements are non-negative real numbers and whose off-diagonal elements are zero. The diagonal elements $\lambda_1, \lambda_2, \ldots, \lambda_{N_{min}}$ denotes the i^{th} singular value of $\mathbf{H}$, and $\lambda_1 \geq \lambda_2 \geq \cdots \geq \lambda_{N_{min}} > 0$, where $N_{min} = min(N_T, N_R)$.

The MIMO channel can then be represented as a parallel channel [85] based on the ordered singular value λ_i as

$$\tilde{y}_i = \lambda_i \tilde{x}_i + \tilde{\eta}_i, \qquad i = 1, \cdots, N_{min} \tag{2.12}$$

and

$$\begin{aligned} \tilde{\mathbf{x}} &= \mathbf{V}^H \mathbf{x}, \\ \tilde{\mathbf{y}} &= \mathbf{U}^H \mathbf{y}, \\ \tilde{\eta} &= \mathbf{U}^H \eta. \end{aligned}$$

Substituting (2.11) into (2.9), we can get

$$C = \max_{p_i : \sum_i p_i \leq P} \sum_{i=1}^{N_{min}} \log(1 + \frac{\lambda_i^2 p_i}{\sigma_\eta^2}), \tag{2.13}$$

The transmitting powers are allocated to each sub-channel based on their strength according to the water-filling strategy,

$$\frac{p_i}{P} = (0, \mu - \frac{\sigma_\eta^2}{\lambda_i^2 P})^+ \tag{2.14}$$

where $(A)^+ = \max(0, A)$, and μ is the waterfilling level which should be chosen so that

the total power constraint is satisfied:

$$\sum_{i=1}^{N_{min}} (\mu - \frac{\sigma_\eta^2}{\lambda_i^2 P}) = 1. \tag{2.15}$$

Therefore, the maximum channel capacity can be obtained as:

$$C_{max} = \sum_{i,p_i>0} \log(1 + \frac{p_i \lambda_i^2}{\sigma_\eta^2}) \tag{2.16}$$

2.5.3 Error Model

In a realistic scenario, however, the CSI is generally imperfect. The receive sensor node can estimate the CSI, *i.e.*, the matrix $\mathbf{H}$, using training sequences, *e.g.*, pilot symbols. Basically there are two ways [7] to get CSIT. The transmit sensor nodes can estimate the channel using the signals received in the reverse link, and use it as an estimate in the forward link, because of the channel reciprocity principle. During the procedure of estimation, estimation error will be introduced without doubt. Suppose the estimation is unbiased, the estimated CSI, $\hat{\mathbf{H}}$ can be formulated as

$$\hat{\mathbf{H}} = \mathbf{H} + \xi \tag{2.17}$$

where ξ is the estimation error. The entries of ξ are assumed to be i.i.d. and zero-mean circularly symmetric complex Gaussian. ξ is independent from the real channel realization. The alternate solution is to obtain the CSI through a feedback channel from the receiver to the transmitter. Besides the Gaussian estimation error at the receiver, due to the finite capacity of the feedback channel, the channel response has to be quantized, which will introduce the another quantization noise to the CSIT.

We will focus on the Gaussian estimation error in the following analysis, and we make

the following assumption.

- The transmit sensor nodes have a total power constraint P, however, they can adapt their power allocation according to the channel fading so as the maximize capacity. The power constraint condition can be mathematically represented as,

$$E(P) = E(tr(Q)) \leq \bar{P}. \tag{2.18}$$

- Either there exists a perfect and instantaneous feedback channel from the receiver to the transmitter, or the delay from the obtaining reverse-channel information to apply the information to the forward-link is negligible. So the only error we consider is the estimation error in (2.17).

2.5.4 Channel Capacity with imperfect CSIT

When there is error in the estimation as discussed in section 2.5.3, what the transmitter knows is the estimated channel matrix $\hat{\mathbf{H}}$ in (2.17). Hereby, the decomposition of the MIMO channel and the application of water-filling strategy in section 2.5.2 are both based on $\hat{\mathbf{H}}$, which contains zero-mean Gaussian Noise. Apparently, the singular value $\hat{\lambda}_i$ obtained from $\hat{\mathbf{H}}$ will be different from λ_i. Consequently, the maximum channel capacity in (2.16) is no longer tenable because the power allocation is not optimized. We will show how the estimation error impact the channel capacity in section 2.6.

2.6 Numerical Results and Discussions

Numerical results are presented to show how Gaussian estimation errors degrade the channel capacity in i.i.d. Rician fading MIMO channel based on Monte-Carlo simulations.

Two MIMO systems, where $N_T = N_R = 3$ and $N_T = N_R = 6$, respectively were sim-

ulated. The MIMO channels were treated as 9 and 36 i.i.d. single-input-single-output (SISO) Rician channels applying the Jakes's model [73] [44].

In Figure 2.2, we compare the average channel capacity using equal power allocation, water-filling strategy with perfect CSIT, and water-filling strategy with channel estimation error as $\sigma_\xi^2 = 0.1, 0.25, 0.5, 1$ respectively in a $N_T = 3, N_R = 3$ MIMO system with the Rician fading parameter as $K = 10$ for all the independent $3 \times 3 = 9$ sub-channels, and f_d is randomly chosen from $0 \sim 30Hz$ for sub-channels.

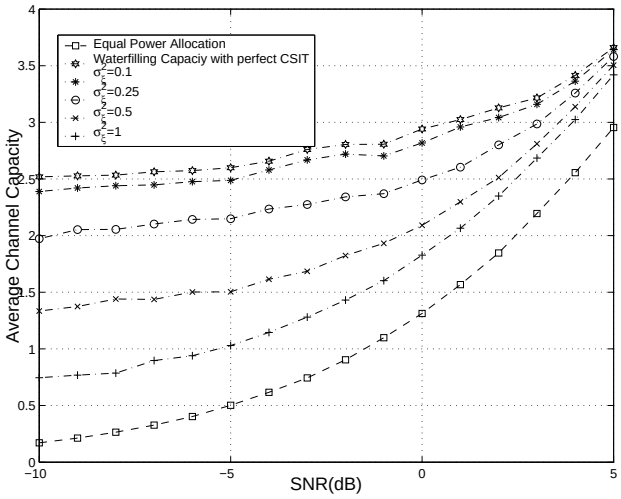

Figure 2.2. Average Channel Capacity for 3×3 MIMO with Rician fading.

We can see clearly that the water-filling scheme performs much better than the equal power allocation scheme, which does not need CSIT, even with estimation error, especially at the low SNR. At high SNR, the difference between water-filling and equal power allocation scheme becomes slimmer.

We then set the Rice factor $K = 0$ for all the sub-channels, which means it is Rayleigh fading. The results are shown in Figure 2.3.

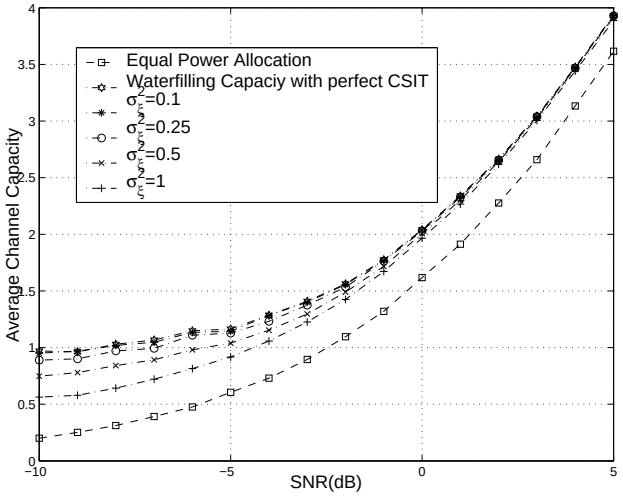

Figure 2.3. Average Channel Capacity for 3×3 MIMO with Rayleigh fading.

For Rayleigh fading MIMO channel, channel capacity is more sensitive to the SNR, but less sensitive to the estimation error.

Figure 2.4 2.5 show the results of the simulation of $N_T = N_R = 6$ system.

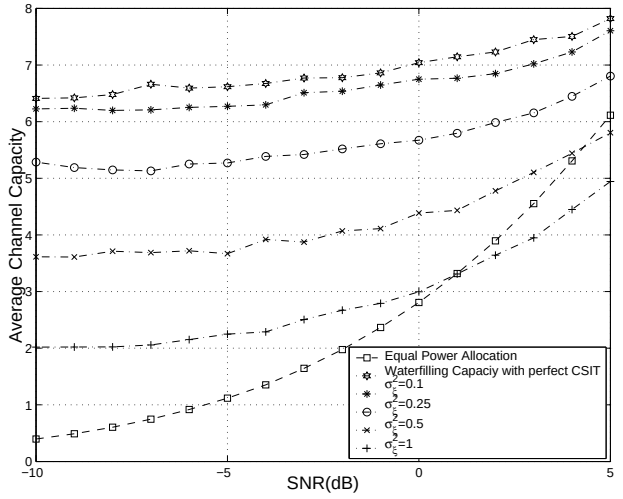

Figure 2.4. Average Channel Capacity for 6×6 MIMO with Rician fading.

We notice that the average channel capacities of equal power allocation strategy are larger than the ones of water-filling strategy at high SNR. When we perform the water-filling

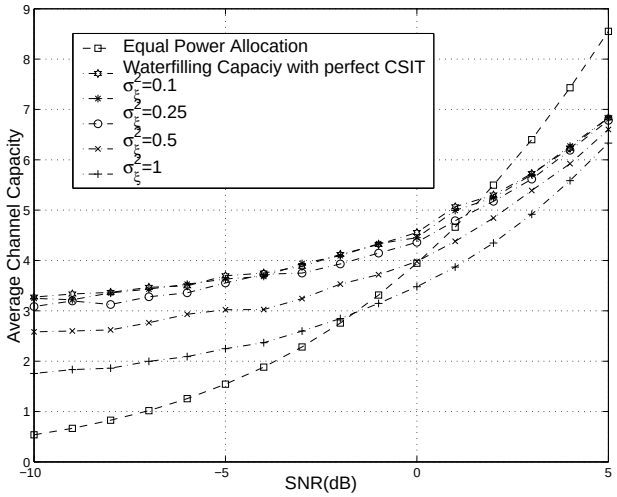

Figure 2.5. Average Channel Capacity for 6×6 MIMO with Rayleigh fading.

scheme, some of the decomposed parallel channels may not be assigned any power, so that some of the diversity gain is lost.

We compare the average channel capacities of $N_T = N_R = 3$ and $N_T = N_R = 6$ MIMO systems at Figure 2.6. The Rician fading parameters K and f_d for each independent sub-channel are chosen from $0 \sim 10$ and $0 \sim 30Hz$ respectively.

Without any doubt, the average channel capacity of the $N_T = N_R = 6$ MIMO system is much larger than the one of the $N_T = N_R = 3$ MIMO system.

Figure 2.7 shows the average channel capacities get from $N_R = 3, N_T = 6$ and $N_R = 6, N_T = 3$ MIMO systems.

For equal power allocation algorithm, the channel capacities for the two systems are exactly the same. However, for water-filling strategy, more gains can be obtained from the receiving part.

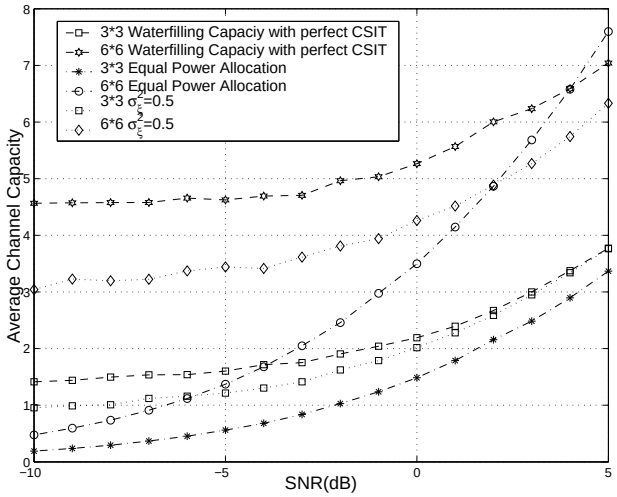

Figure 2.6. Average Channel Capacities for 6×6 and 3×3 MIMO systems.

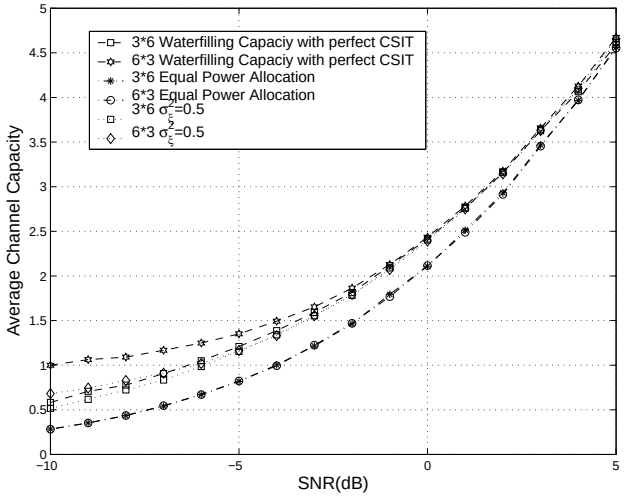

Figure 2.7. Average Channel Capacities for 3×6 and 6×3 MIMO systems.

2.7 Chapter Summary

Virtual MIMO structure is very attractive to wireless sensor network due to its potential huge diversity gain. Wireless sensor network is power constraint, however, with CSIT, water-filling algorithm can be applied to optimize the power allocation in each sub-channel of the MIMO system based on the estimated channel matrix $\mathbf{H}$, so as to maximize the channel capacity of the system even in deep fading scenario. However, in reality, both the estimation error and the quantization noise will be introduced when estimate the channel.

In this chapter, we first discuss the virtual MIMO structure in wireless sensor network, then set up the MIMO system model focused on one-hop inter-cluster transmission. Afterwards, the error model of the channel estimation is investigated, and how the estimation error will impact the optimal water-filling strategy is analyzed. Numerical results were presented based on the Monte-Carlo simulations.

CHAPTER 3

UWB SENSOR NETWORKS IN HOSTILE ENVIRONMENT

Interferences due to the hostile environment (e.g. jammer) and the Multi-User Access are critical factors affecting performance of the wireless sensor networks. In this paper, we study a hybrid Frequency Hopping/Time Hopping-Pulse Position Modulated (FH/TH-PPM) UWB for wireless sensor networks in hostile environment with partial-band(PB) tone interference. FH and TH are both used to get as much diversity gain as possible. Theoretical analysis is made for the bit error rates performance in the presence of multitone/pulse (tone in frequency domain and pulse in time domain) interference and Multi-User Interference. We also derived theoretical performance formula when the low duty-cycle in UWB system and the large number of sensor nodes in a wireless sensor networks are considered.

3.1 Introduction

Wireless sensor networks are becoming more popular for an ever increasing range of applications with improvements in device size, power control, communications and computing technology. Since 2002 there has been great increasing popularity of commercial applications based on Ultra WideBand. This in turn has ignited interest in the use of this technology for sensor networks. Actually, UWB systems have potentially low complexity and low cost; have a very good time domain resolution, which facilitates location and tracking applications. So, UWB wireless sensor networks are promising.

One of the most important applications of wireless sensor network is in battle field, which means there exist hostile interferences. Frequency Hopping (FH) technology offers an improvement in performance when the communication systems is attacked by hostile

interference and reduce the ability of a hostile observer to receive and demodulate the communication signal. This kind of inherent property finds it a potential position in the UWB sensor networks. Based on the UWB definition released by the FCC (FCC, 2002) that a signal is UWB if its bandwidth exceeds 500 MHz, the overall 7.5 GHz bandwidth, that is, frequencies in the range 3.1 GHz to 10.6 GHz as based on the FCC ruling, can be split into smaller frequency bands of at least 500 MHz each. This character inspired us to design a hybrid FH/TH-PPM UWB system.

Sensor Network communication systems have to be multi-user accessible, which means different users/sensor nodes are allowed to share the same physical medium for transmitting and receiving different data flows. In TH-UWB, the spectrum of the impulse radio signal is usually shaped by encoding data symbols using TH sequences, which are typically described as pseudo-random PN codes. These same sequences can also serve as users' signatures and ensure access to the medium to multiple users. Therefore, this so called Time Hopping Multiple Access (THMA) technology will be a reliable choice in this case. However, in a realistic scenario where systems cannot achieve ideal synchronization, multi-user interference (MUI) will be another crucial factor besides the previous mentioned hostile interference to affect the system performance. Clearly, the simple Signal-to-Noise-Ratio (SNR) is less than enough to give a comprehensive performance evaluation for sensor networks. Therefore, Signal-to-Interference-plus-Noise-Ratio (SINR) should be analyzed instead.

Several efforts have been made in the recent past for evaluating the effect of MUI on symbol error rate with single-user reception in an AWGN channel [38, 103]. However, hostile jammer is considered in none of them, which would be challenged in this paper. For example, a TH-UWB sensor network, which is set up in a hostile environment, it is feasible for the enemies to estimate the shape of a pulse. Therefore, a repeated-imitated-pulses intruder will be sent out to degrade the performance of the network. The main

contribution of this paper, we put the hostile interference along with the MUI into consideration, and through the precise analysis a closed-form performance analysis expression can be got.

The rest of this chapter is organized as follows. The system models, including the transmission, channel and receiver, will be introduced in Section 3.2. The MUI and hostile interference will be studied in Section 3.3 and Section 3.4 respectively, and the SINR and closed-form BER will be derived as well. Numerical results and comparisons will be present in Section 3.5; and conclusions are made in Section 3.6.

3.2 System Models

In the proposed system, there are N_F non-overlapping FH bands, each with bandwidth B_h where B_h is the bandwidth required to transmit a TH-PPM signal in the absence of FH. Let $s^k(t)$ denotes the k-th user's signal at time t in this FH/TH-PPM UWB system with totally N_u users, and it takes the form

$$s^k(t) = \sqrt{\frac{E_b}{N_s}} \sum_{j=-\infty}^{+\infty} c_j^{fh}(k) p[t - jT_f - c_j^{th}(k)T_c - d_j(k)\delta]) \tag{3.1}$$

where $p(t)$is a chip waveform, which can take arbitrary time-limited pulse shapes proposed specifically for UWB communication systems, and is normalized to satisfy $\int_{-\infty}^{+\infty} p^2(t)dt = 1$. The notations and parameters are:

- N_s is the number of pulses used to transmit a single information bit. T_f is the time duration of a frame. In general case, $N_s \geq 1$ pulses carry the information of one bit. The bit duration T_b should satisfy, $T_b \geq T_f N_s$.

- E_b is the energy per information bit. $\sqrt{\frac{E_b}{N_s}}$ is the normalized energy in each symbol.

- $c_j^{th}(k)T_c$ is the time shift introduced by the TH code. T_c is the chip duration. $c_j^{th}(k)$ is the j-th coefficient of the TH sequence used by user k; it is pseudo-random with each element take an integral in the range $[0, N_h - 1]$, where N_h is the number of hops. $T_c \leq T_f/N_h$ should be satisfied.

- The $d_j(k)\delta$ term represents the time shift introduced by PPM modulation. In our system, 2PPM is only considered. Therefore, $d_j(k)$ represents the j-th binary data bit (0 or 1) transmitted by the k-th user; δ is the PPM shift.

- $c_j^{fh}(k) = \sqrt(2)cos(2\pi f_k j)$ is the k-th user's spreading code during j-th frame.

Notice that each symbol chooses one of the N_F sub-bands to transmit the signal, however, in each sub-band, the transmitted signal is TH-2PPM.

In wireless sensor networks, sensor nodes have two states, i.e., active communication status and idle status. In order to save energy, sensor nodes choose to be idle for most of the time. The number of nodes who are actually in the status of active communication is unknown. However, the total number of sensor nodes in the network and the access rate λ, i.e., the rate that a node in the communication status, for each node are assumed to be known. Clearly, the event of status of sensor node is a Bernoulli distribution with mean as λ and variance as $\lambda(1 - \lambda)$. Assume there are N_U sensor nodes in a network, each one of them chooses to be idle or active independently. Therefore, the number of sensor nodes who are in active communication status, N_u^T, can be seen as the sum of N_U independent, identically distributed Bernoulli random variable, which is a Binomial distribution. Usually N_U is very large, we can approximate the Binomial dis-

tribution to a Gaussian random variable with the mean $N_U\lambda$ and variance $N_U\lambda(1-\lambda)$, as

$$f_{N_u^T}(n_u^t) = \frac{1}{\sqrt{2\pi N_U\lambda(1-\lambda)}} e^{-(n_u^t - N_U\lambda)^2/2N_U\lambda(1-\lambda)} \tag{3.2}$$

For the N_u^T users, they randomly choose one of the sub-bands to transmit the signal according to $c_j^{fh}(k)$ symbol by symbol. It is also a Binomial random variable with the coefficient $1/N_F$. To simplify the problem, we assume that the users are distributed optimally, so the number of users share the same channel, N_u, should be expressed as

$$N_u = N_u^T/N_F. \tag{3.3}$$

Assume over one T_f, N_u users' signals are simultaneously transmitted over a channel with L_c paths [23], the composite waveform at the output of the receiver antenna maybe written as

$$r(t) = \sum_{k=1}^{N_u}\sum_{l=1}^{L_c} \alpha_l^{(k)} s_j^{(k)}(t-\tau_l^{(k)}) + n(t) + I(t) \tag{3.4}$$

where $n(t)$ is the additive Gaussian Noise withe two-sided power spectral density $N_0/2$, $I(t)$ is the hostile jammer interference, $\alpha_l^{(k)}$ and $\tau_l^{(k)}$ are the attenuation and the delay affecting replica of the k-th user's signal traveling through the l-th path. In writing (3.4), we have implicitly assumed a static channel, meaning the $\alpha_l^{(k)}$ and $\tau_l^{(k)}$ are either fixed or vary so slowly that they are practically constant over several bits.

Consider $s^{(1)}(t)$ to be the desired user, all the other $N_u - 1$ users signals are interference signals. We make assumptions

- The reference transmitter and receiver of a reference link are perfectly synchronized under the coherent detection hypothesis;

- A dominant path exists that conveys the major part of the desired user's energy [58];

the decision statistic over the 1-st user's j-th symbol is obtained as

$$z_j = \int_{jT_f}^{(j+1)T_f} r(t)v(t - \tau_1^{(1)} - jT_f - c_j^{(1)}T_c)dt, \tag{3.5}$$

where $v(t) = p(t) - p(t - \delta)$ is the correlation template waveform.

Afterwards, a simple hard decision of the information bit based on $z_j, j = 0, 1, \ldots, N_s - 1$ will be made by majority law.

3.3 Multi-User Interference Analysis

In this section, we will first focus on the analysis of MUI with the absence of hostile jammer interference. We assume there is no inter-channel-interference. Therefore, the received signal of 1-st user's j-th symbol can be expressed as:

$$r_j(t) = r_j^{(1)}(t) + r_{j,mui}(t) + n(t) \tag{3.6}$$

where $r_{j,mui}(t)$ is the MUI contribution at the receiver input. If the users are many and have comparable powers, we can approximate the MUI as a white Gaussian process by the central limit theorem [99] and, as such, it can be lumped into the additive Gaussian

Noise,

$$w_{tot}(t) = r_{j,mui}(t) + n(t) \tag{3.7}$$

and $w_{tot}(t)$ is still a white Gaussian process. Correspondingly, the minimum error probability can be achieved by computing (3.5).

However, we still need to evaluate the energy of the MUI. Since the system is asynchronous, we need to consider all cases where a pulse originated by any of the transmitters but TX1, is detected by the receiver. First of all we need to analyze the noise provoked by the presence of one alien pulse at the output of the receiver by using the similar method as in[6],

$$mui^{(k)}(\tau^{(k)}) = \sqrt{E_{RX}^{(k)}} \int_0^{T_c} p(t - \tau^{(k)}) v_t dt \tag{3.8}$$

where, $E_{RX}^{(k)} = \alpha^{(k)}(E_b/N_s)$, and here we suppose $\alpha^{(k)} = 1 \ \forall k$.

Since $\tau^{(k)}$ is uniformly distributed over $[0, T_f)$, however, the region the MUI noise can affect to the desired user , is only at $[-T_p, T_c]$, with $T_c = 2T_p$[6]. Hence,

$$\sigma^2_{mui^{(k)}} = \frac{1}{T_f} \int_{-T_p}^{T_c} \left(\sqrt{E_{RX}^{(k)}} \int_0^{T_c} p(t - \tau^{(k)}) v(t) dt \right)^2 d\tau^{(k)} \tag{3.9}$$

and cumulate all the $N_u - 1$ interference sources, the total MUI energy is

$$\sigma^2_{mui} = \frac{1}{T_f} \sum_{k=2}^{N_u} E_{RX}^{(k)} \left(\int_0^{T_f} \left(\int_0^{T_c} p(t - \tau^{(k)}) v(t) dt \right)^2 d\tau^{(k)} \right) \tag{3.10}$$

Since all the delays, τ, are identically distributed, and under the hypothesis of perfect

power control, e.g., $E_{RX}^{(k)} = E_{RX}\ \forall k$,

$$\sigma_{mui}^2 = \frac{E_{RX}}{T_f} \sum_{k=2}^{N_u} \left(\int_0^{T_f} \left(\int_0^{T_c} p(t-\tau)v(t)dt \right)^2 d\tau \right) \tag{3.11}$$

Define σ_M^2 as

$$\begin{aligned} \sigma_M^2 &= \int_0^{T_f} \left(\int_0^{T_c} p(t-\tau)v(t)dt \right)^2 d\tau \\ &= \int_0^{T_f} \left(\int_0^{T_c} p(t-\tau)\left(p(t) - p(t-\delta)\right)dt \right)^2 d\tau \\ &= \int_{-T_p}^{T_f} \left(R_0(\tau) - R_0(\tau+\delta)\right)^2 d\tau \end{aligned} \tag{3.12}$$

and (3.10) becomes

$$\sigma_{mui}^2 = \frac{E_{RX}}{T_f}(N_u - 1)\sigma_M^2 \tag{3.13}$$

Therefore, the SIR_{mui} over one symbol can be expressed as:

$$SIR_{mui} = \frac{T_f}{(N_u - 1)\sigma_M^2}. \tag{3.14}$$

Let SNR_{ref} denotes the equivalent signal to noise and MUI ratio over one symbol, it can be written as

$$SNR_{ref} = (SNR_n^{-1} + SIR_{mui}^{-1})^{-1} \tag{3.15}$$

where SNR_n are the signal to noise ratio over one symbol.

Hence,

$$\begin{aligned} SNR_{ref} &= \left(\left(\frac{E_{RX}}{N_0} \right)^{-1} + \left(\frac{T_f}{(N_u - 1)\sigma_M^2} \right)^{-1} \right)^{-1} \\ &= \frac{T_f}{N_s T_f + (N_u - 1)\sigma_M^2 \left(\frac{E_b}{N_0} \right)} \left(\frac{E_b}{N_0} \right) \end{aligned} \tag{3.16}$$

where $E_b/N_0$is the system SNR.

We can also get the equivalent variance of $w_{tot}(n)$,

$$N_0' = N_0 + \frac{(N_u - 1)\sigma_M^2 E_b}{N_s T_f} \tag{3.17}$$

3.4 Performance Analysis with Multitone/pulse Interference

In this section, the SIR for the hostile interference part is obtained. As previously mentioned, in a hostile environment, which is a common case for sensor networks, it is feasible for an enemy to estimate/detect the pulse waveform, furthermore, send the imitational waveform to interfere the communication system. However, it is not economy or efficient for the interference to cover all the frequency bandwidth. So, what we study here is a multitone/pulse (tone in frequency domain; and pulse in time domain) interference, which implies that the jamming signal consists of one or more tones/sub-bands transmitted within the total bandwidth; and it has the same pulse shaper as the transmitted 2-PPM signal does.

We make the following assumptions:

- The multitone/pulse interference has a total power P_J, which is transmitted in a total of q equal power interfering tones spread randomly over the spread spectrum

bandwidth;

- The time duration for the interference pulse is the same as the time duration of the transmitted signal pulse $p(t)$, which is denoted as T_p. To simplify the problem, we suppose $T_c = 2T_p$ and $\delta = T_p$. The hop period of the interference is also T_p, and each hop is independent;

- The multitone/pulse interference can catch the signal pulse with the perfect timing. We consider the scenario that there is at most one interference per FH subband. Hence, in one hop, the probability that a FH band contains an interference tone/pulse is q/N_F. Observe the transmitted signal as in (3.1), the signal hops both in the frequency domain and in the time domain symbol by symbol. Therefore, our analysis will first focus on one symbol.

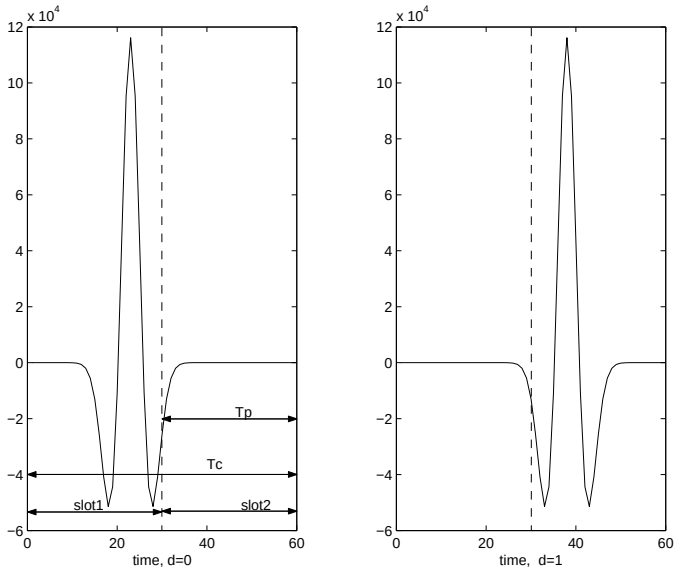

Figure 3.1. An example of the waveform of a 2-PPM signal.

For one symbol, no matter what $c_j^{fh}(k)$ and $c_j^{th}(k)$ are, it is a 2-PPM signal shown as in Fig 3.1. The left one is the waveform when $d_j(k) = 0$, and the right one is the waveform when $d_j(k) = 1$. We partition the symbol duration as two time slots, hence, for the multi-tone/pulse interference, there are two hops. And because in each hop, it is independently distributed, there should be totally four cases with regard to the jammer interference for each symbol:

1. *Case1.* There is no jammer interference in either of two slots, and the probability of case1 is

$$P\{case1\} = (1 - \frac{q}{N_F}) \cdot (1 - \frac{q}{N_F}). \tag{3.18}$$

2. *Case2.* There is jammer interference in each slot, and the probability of case2 is

$$P\{case2\} = \frac{q}{N_F} \cdot \frac{q}{N_F}. \tag{3.19}$$

3. *Case3.* There is one and only one jammer interference pulse, and it is at the same slot as the signal pulse. The probability of case3 is

$$P\{case3\} = (1 - \frac{q}{N_F}) \cdot \frac{q}{N_F}. \tag{3.20}$$

4. *Case4*. There is one and only one jammer interference pulse, and it is not at the same slot as the signal pulse. The probability of case4 is

$$P\{case4\} = (1 - \frac{q}{N_F}) \cdot \frac{q}{N_F}. \tag{3.21}$$

The received signal of the j-th symbol of 1-st user can be expressed as:

$$r'_j(t) = r^1_j(t) + I_{jammer}(t) + w_{tot}(t); \tag{3.22}$$

where $r^k_j(t)$ and $I_{jammer}(t)$ are the jammer interference contributions at the receiver input, and $w_{tot}(t)$ accounts for both the thermal and MUI noise contributions, and is still a white Gaussian process as proved in Section 3.3. Hence, a maximum a posteriori (MAP) approach can be adopted here to get the minimum error probability. For different cases of the jammer interference, the detection boundaries are shown in Fig. 3.2.

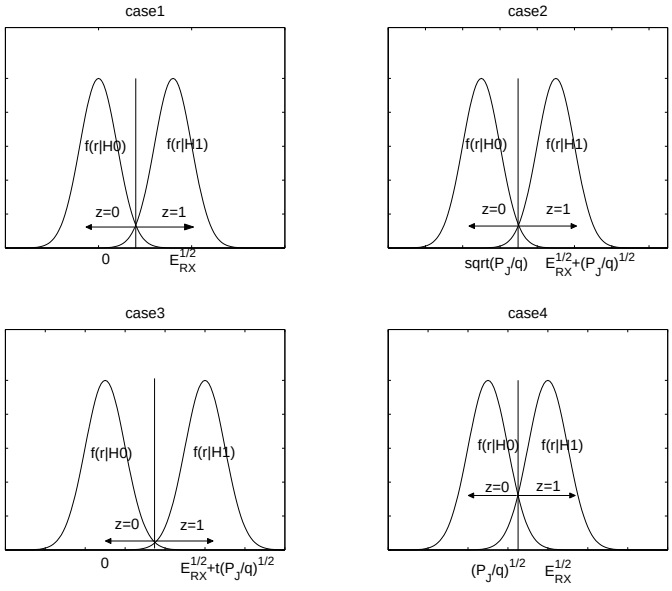

Figure 3.2. The MAP detection rule for all the cases.

Hence, we can get the $SINR_{jammer}$ straightforwardly.

- For case1 and case2,

$$SINR_{jammer|case1,2} = \frac{E_{RX}}{N_0'}. \tag{3.23}$$

- For case 3,

$$SINR_{jammer|case3} = \frac{(\sqrt{E_{RX}} + \sqrt{\frac{P_J}{q}})^2}{N_0'}. \tag{3.24}$$

- For case 4,

$$SINR_{jammer|case4} = \frac{(\sqrt{E_{RX}} - \sqrt{\frac{P_J}{q}})^2}{N_0'}. \tag{3.25}$$

For 2-PPM signal the error probability is [6],

$$Pr = Q(\sqrt{SNR_{spec}}). \tag{3.26}$$

Apply (3.17) and (3.23) to (3.25) into (3.26), we can derive,

- For case1 and case2,

$$pr_{s|c1,2} = Q(\sqrt{\left(\frac{\frac{E_b}{N_s}}{N_0'}\right)}); \tag{3.27}$$

- For case 3,

$$pr_{s|c3} = Q(\sqrt{\left(\frac{(\sqrt{\frac{E_b}{N_s}} + \sqrt{\frac{P_J}{q}})^2}{N_0'}\right)}); \tag{3.28}$$

- For case 4,

$$pr_{s|c4} = Q(\sqrt{\left(\frac{(\sqrt{\frac{E_b}{N_s}} - \sqrt{\frac{P_J}{q}})^2}{N_0'}\right)}). \tag{3.29}$$

Removing the conditioning on cases, we get

$$\begin{aligned} Pr_s' &= \left(\left(\frac{N_F - q}{N_F}\right)^2 + \left(\frac{q}{N_F}\right)^2\right) Q(\sqrt{\left(\frac{\frac{E_b}{N_s}}{N_0'}\right)}) \\ &+ \left(\frac{N_F - q}{N_F}\right)\left(\frac{q}{N_F}\right)(Q(\sqrt{\left(\frac{(\sqrt{\frac{E_b}{N_s}} + \sqrt{\frac{P_J}{q}})^2}{N_0'}\right)}) \\ &+ Q(\sqrt{\left(\frac{(\sqrt{\frac{E_b}{N_s}} - \sqrt{\frac{P_J}{q}})^2}{N_0'}\right)})). \end{aligned} \tag{3.30}$$

Considering only N_u is a random variable, we should take (3.2) and (3.3) into (3.30),

$$\begin{aligned} Pr_s = \frac{1}{N_F\sqrt{2\pi N_U\lambda(1-\lambda)}} \int_1^{N_U} Pr_s' \\ e^{-(n_u - N_U\lambda)^2/2N_U\lambda(1-\lambda)} dn_u \end{aligned} \tag{3.31}$$

After we got the symbol error rate Pr_s, it is easy for us to obtain the bit error rate Pr_b by majority law.

$$Pr_b = \sum_{k=\lceil \frac{N_s}{2} \rceil}^{N_s} C_{Ns}^k Pr_s^k (1 - Pr_s)^{N_s - k} \tag{3.32}$$

where $\lceil\ \rceil$ is the ceiling operation, and C_{Ns}^k is an N_s-choose-k Binomial coefficient, i.e., $C_{Ns}^k = \frac{k!(N_s-k)!}{N_s!}$.

3.5 Numerical Results and Comparisons

Table 3.1. Parameters of the example FH/TH-PPM UWB system

Parameter	Notation	2^{nd}-order mono-cycle
shaping factor for the pulse	ϵ	$0.25ns$
time shift introduced by PPM	δ	$0.5ns$
pulse duration	T_p	$0.5ns$
frame duration	T_f	$8ns$
chip duration	T_c	$1ns$
number of hops	N_h	6

The parameters of the example UWB systems are listed in Table 3.1.

- The discussion on N_s;

We fix $N_F = 20$, $q = 8$, $N_u = 10$ and the energy of the signal and jammer interference ratio $E_b/P_J = 5dB$, and compare the Symbol Error Rate (SER) and Bit Error Rate (BER) among $N_s = 1, 3, 5, 7$. The results are shown in Figure. 3.3 and Figure. 3.4 respectively. For SER, because, the more symbols used to transmit one bit, the energy for each symbol is less, SER is increasing when the N_s increases.

However, BER is more meaningful here, and obviously, the more symbols we used to transmit one information bit, the better performance we can achieve. The curves drop quickly from $SNR = 0dB$ to $15dB$, however, after $15dB$, become flat, which caused by the jammer interference.

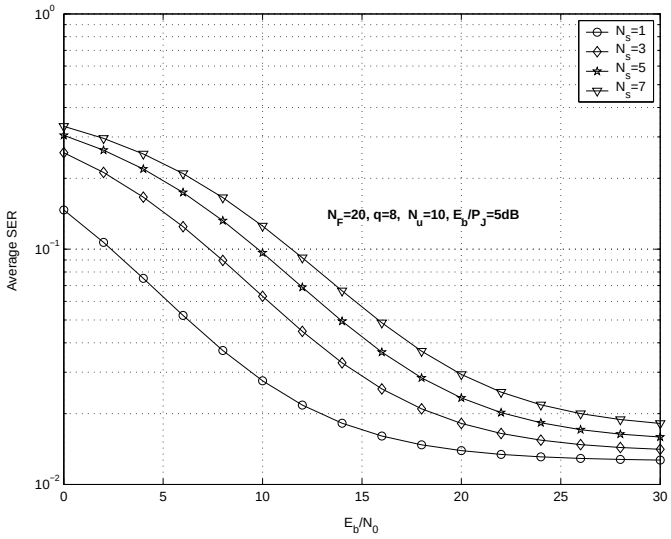

Figure 3.3. The average SER for different N_s.

- The discussion on E_b/P_J;

  We set $N_F = 20$, $N_s = 3$, $q = 8$, and $N_u = 10$, and compare the SER and BER among $E_b/P_J = 0, 5, 10dB$. Figure. 3.5 and Figure 3.6 show the results. For both SER and BER, larger E_b/P_J can guarantee better performance. From $E_b/P_J = 5dB$ to $E_b/P_J = 10dB$, the performance gain is very limited, the reason of which is when E_b/P_J is higher than some better threshold, the jammer interference is too weak to give any impact to the system.

- The discussion on q;

  N_F, N_s, N_u and E_b/P_J are fixed at 20, 5, 10 and $5dB$ respectively.We try to evaluate the performance for $q = 2, 8, 18$. At the first glance, larger q may be

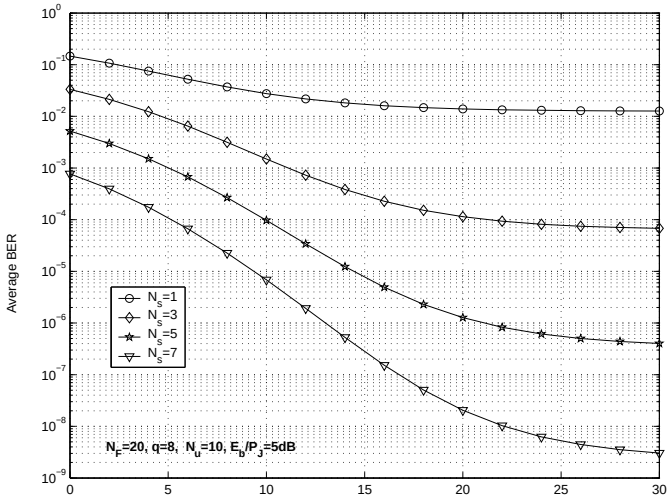

Figure 3.4. The average BER for different N_S.

thought to yield worse performance, because large q means the probability that a jammer interference bumps the information signal is higher. However, we need to notice, high q also means the energy of the jammer interference for each sub-band is less, because the total jammer interference power is fixed. We can get the same conclusion in the Figure. 3.7 and Figure. 3.8. The worst and best performances are get at $q = 2$ and $q = 8$ respectively.

- The discussion on N_F;

  We evaluate the performance for $N_F = 1, 5, 10, 20$ when $N_s = 1$, and the number of users who are at communication status is 100. We need to evaluate how partitioning N_F can decrease the MUI, therefore, we set it as a jammer interference free channel. Obviously, Figure. 3.9 shows that we can get better performance when N_F is larger. Considering, more sub-bands partitioned means more cost, the N_F should be set at an appropriate value as long as the Quality of Service (QoS) is satisfying.

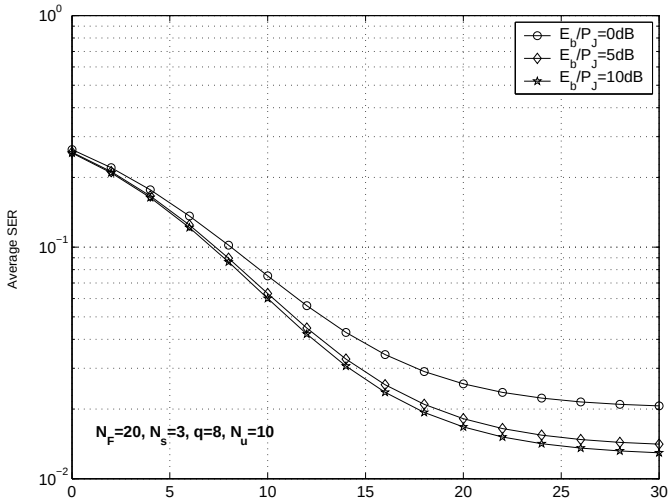

Figure 3.5. The average SER for different E_b/P_J.

- The discussion on N_u;

  We set $N_F = 20$, $q = 8$, $N_s = 5$ and $E_b/P_J = 5dB$. N_u is equal to $5, 10, 15, 20$ respectively to get different performance, which are shown in Figure. 3.10 and Figure. 3.11. At high SNR, the performance is degraded quickly when N_u becomes larger. That is because the MUI is related with E_b under the assumption that each user has comparable power.

- The discussion on λ;

  We proved in Section 3.2 that the N_u is approximately a Gaussian RV.With known N_U, the number of sensor nodes in the wireless sensor network, but unknown N_u, the number of users that would share the same sub-band, we need to calculate the SER as in (3.31). We set $N_U = 10,000$, N_F is set as 20 and we assume the users are optimally distributed. For different access rate, $\lambda = 0.01$ and $\lambda = 0.02$, the performances are shown in Figure 3.12 and Figure. 3.13, we can see though the N_U are the same, the difference in λ would yield totally different performance.

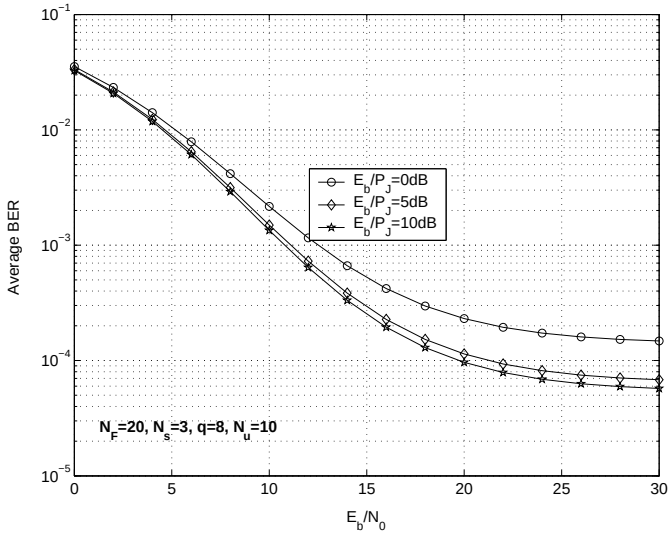

Figure 3.6. The average BER for different E_b/P_J.

3.6 Chapter Summary

In this chapter, we make an performance analysis with the presence of the multi-tone/pulse jammer interference and multi-user interference based on the hybrid FH/TH-PPM-UWB system. We get an accurate expressions of SER and BER with the presence of MUI and hostile jammer interference. We evaluate the performances for different number of symbols to carry one information bit N_s; the signal to jammer interference ratio E_b/P_J; the number of FH sub-bands N_F; the number of tones q of the jammer interference; the number of users sharing the same sub-band N_u; and the total number of users in the wireless sensor networks N_U, and the access rate for each sensor nodes λ, in terms of BER and SER so as to show how these parameters affect to the FH/TH-PPM UWB system.

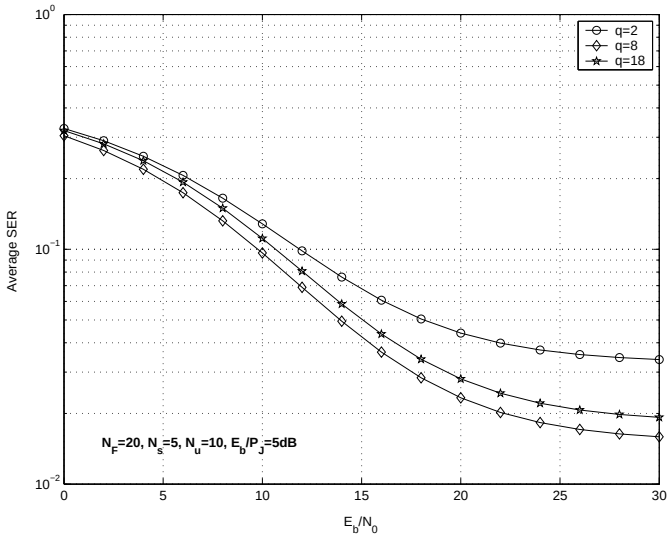

Figure 3.7. The average SER for different q.

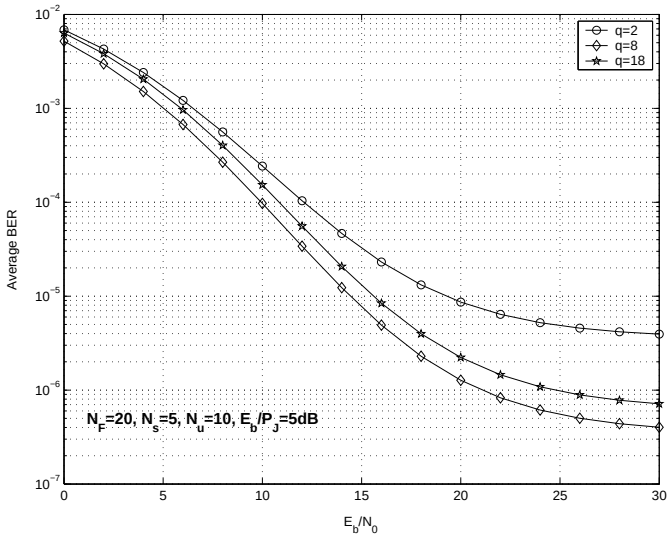

Figure 3.8. The average BER for different q.

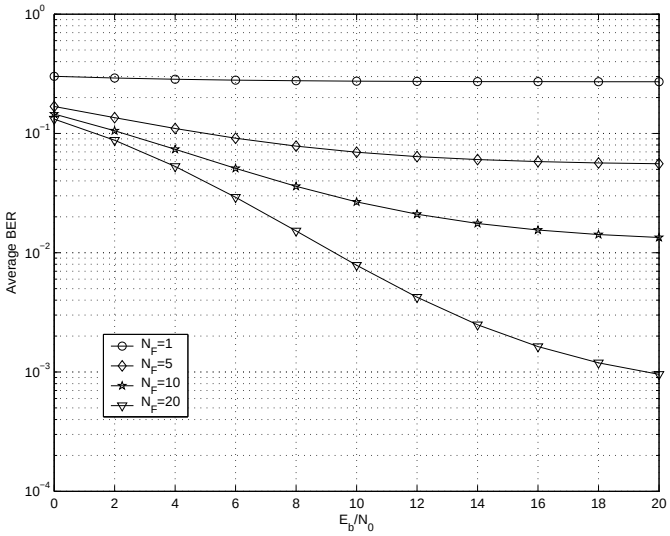

Figure 3.9. The average BER for different N_F.

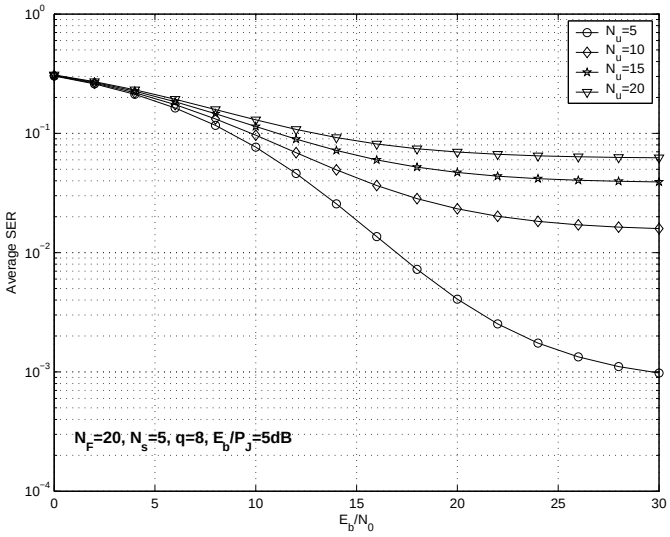

Figure 3.10. The average SER for different N_u.

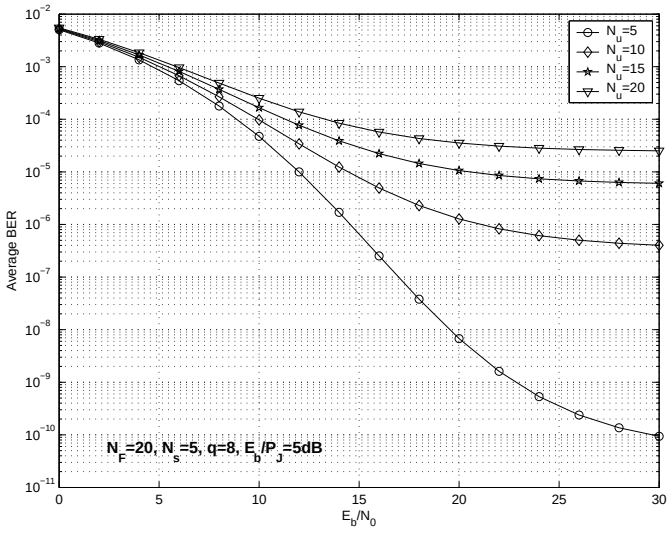

Figure 3.11. The average BER for different N_u.

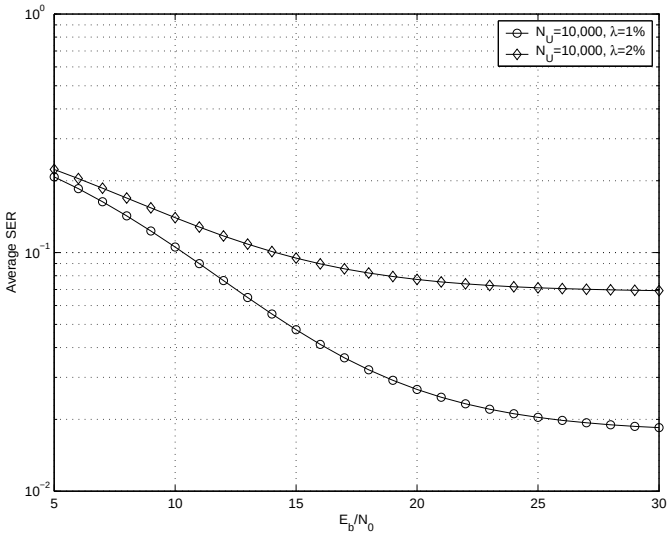

Figure 3.12. The average SER for different λ.

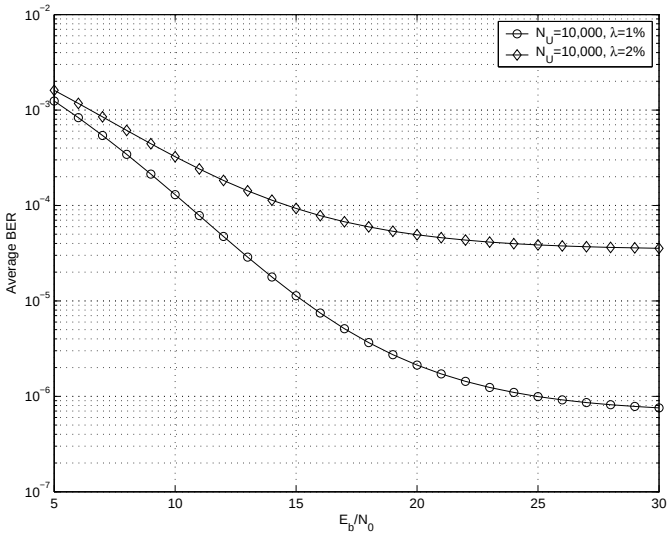

Figure 3.13. The average BER for different λ.

CHAPTER 4

EVENT DETECTION IN WIRELESS SENSOR NETWORKS

The main goal of wireless sensor network is to monitor physical world. Usually, people are more interested in unexpected events. For example, in a scenario of battlefield, people are more interested in the appearance of enemies. If a wireless sensor network is to monitor forest-fire, unusual increasing of the temperature should be a necessary warning to people. Both the appearance of enemies and the unusual increasing of the temperature can be seen as events. Because of the energy constraint of wireless sensor network, the ideal state of wireless sensor network should be event-driven, so that we can power off the communication part at most of the time. Only when certain sensor nodes detect an event, they trigger the communication channel, and transmit the useful information to base-station or headquarters. Therefore, event-detection is one of the key issues for wireless sensor network.

In this chapter we present two approaches of event-detection for wireless sensor network, *double sliding window* and *hybrid event-detection using fuzzy logic system*. We use Berkeley MICA2 motes[35] as our test-bed and evaluate the event-detection approaches based on the acoustic data collected by the test-bed in different experiments.

The remainder of this chapter is organized as follows. the sensor model is given in Section 4.1. The double sliding window and hybrid event-detection based on fuzzy logic system approaches are presented in Section 4.2 and Section 4.3 respectively. Simulation results and discussions are presented in section 4.4. Section 4.5 concludes this chapter.

4.1 Acoustic Sensor Model

Acoustic amplitude sensor node measures sound amplitude at the microphone. Assuming that the sound source is a point source and sound propagation is lossless and isotropic, a root-mean-squared (RMS) amplitude measurement z is related to the sound source position X as

$$z = \frac{a}{\|X - \varsigma\|} + w, \tag{4.1}$$

where a is the RMS amplitude of the sound source, ς is the location of the sensor, and w is RMS measurement noise [53]. In this paper, we use Xbow wireless sensor network professional developer's kit MOTE-Kit for data collection.

4.2 Double Sliding Window event-detection

In [60],the acoustic energy in a fixed period of time is integrated, when it exceeds a threshold, the authors claim a detection of event occurred, as:

$$E_s = \sum_{m=0}^{M-1} |z_{n-m}|^2, \tag{4.2}$$

$$E_s \geq E_{threshold}. \tag{4.3}$$

However, this simple method suffers from a significant drawback; namely, the value of the threshold depends on the sensed signal energy. When there is no event occurring in the sensing range, the sensed signal consists of only noise. The level of the noise power is generally unknown and can change when the environment changes or if unwanted interferers go on and off. Therefore, it is quite difficult to set a fixed threshold. We design a double sliding window algorithm for event-detection so as to alleviate the threshold value selection problem.

The double sliding window event-detection algorithm calculates two consecutive sliding windows of the sensed signal energy. The basic principle is to form the decision variable as the ratio of the total energy contained inside the two windows. Figure 4.1 shows the windows A and B and the response of the ratio m_n to a sensed event. It can be seen that when only noise is sensed the response is flat, since both windows contain ideally the same amount of noise energy.

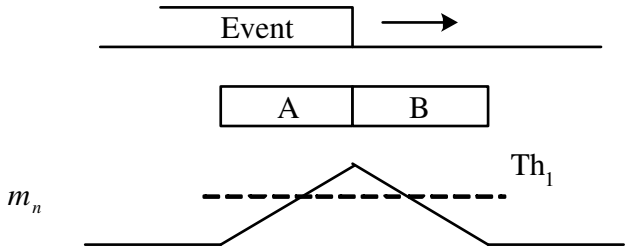

Figure 4.1. The response of the double sliding window event-detection algorithm.

The calculation of the window A and window B value is shown as

$$E_a = \sum_{m=0}^{M-1} |z_{n-m}|^2 , \tag{4.4}$$

$$E_b = \sum_{m=1}^{M} |z_{n+m}|^2 . \tag{4.5}$$

Then the decision variable m_n is

$$m_n = \frac{E_a}{E_b}. \tag{4.6}$$

The advantage of this approach is the decision variable m_n does not depend on the sensed signal energy, but on the ratio of the energy of two consecutive windows.

4.3 Hybrid Event-Detection Based on Fuzzy Logic System

Using the double sliding window algorithm to do event-detection is a good approach. However, if an event continuously appears in the sensing range of a node, the ratio m_n will still be flat. The probability of detection will decrease accordingly. In order to solve this problem, we present a hybrid event-detection algorithm based on fuzzy logic system.

4.3.1 Overview of Fuzzy Logic Systems

Figure 4.2 shows the structure of a fuzzy logic system (FLS) [61]. When an input is applied to a FLS, the inference engine computes the output set corresponding to each rule. The defuzzifer then computes a crisp output from these rule output sets. Consider a p-input 1-output FLS, using singleton fuzzification, *height* defuzzification [61] and "IF-THEN" rules of the form [59]

$$R^l : \text{IF } x_1 \text{ is } F_1^l \text{ and } x_2 \text{ is } F_2^l \text{ and } \cdots \text{ and } x_p \text{ is } F_p^l, \text{ THEN } y \text{ is } G^l.$$

Assuming singleton fuzzification, when an input $\mathbf{x}' = \{x_1', \ldots, x_p'\}$ is applied, the degree of firing corresponding to the lth rule is computed as

$$\mu_{\mathrm{F}_1^l}(x_1') \star \mu_{\mathrm{F}_2^l}(x_2') \star \cdots \star \mu_{\mathrm{F}_p^l}(x_p') = \mathcal{T}_{i=1}^{p} \mu_{\mathrm{F}_i^l}(x_i') \tag{4.7}$$

where $\star$ and $\mathcal{T}$ both indicate the chosen t-norm. There are many kinds of defuzzifiers. In this paper, we focus, for illustrative purposes, on the height defuzzifier [61]. It computes a crisp output for the FLS by first obtaining the height, $\overline{y}^l$, of every consequent set G^l, and, then computing a weighted average of these heights. The weight corresponding to the lth rule consequent height is the degree of firing associated with the lth rule, $\mathcal{T}_{i=1}^{p} \mu_{\mathrm{F}_i^l}(x_i')$,

so that

$$y_h(\mathbf{x}') = \frac{\sum_{l=1}^{M} \overline{y}^l \mathcal{T}_{i=1}^{p} \mu_{\mathrm{F}_i^l}(x_i')}{\sum_{l=1}^{M} \mathcal{T}_{i=1}^{p} \mu_{\mathrm{F}_i^l}(x_i')} \tag{4.8}$$

where M is the number of rules in the FLS. In this paper, we design a FLS for event-detection of wireless sensor network.

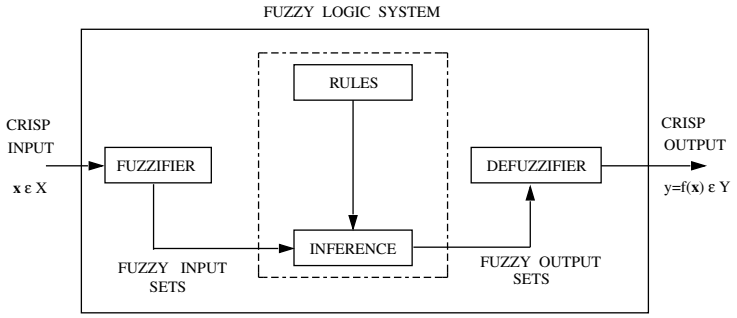

Figure 4.2. The structure of a fuzzy logic system.

4.3.2 Hybrid event-detection algorithm

We have two inputs for the FLS:*the accumulated signal energy E_s in a fixed period of time* and *the ratio of the accumulated signal energy in two consecutive sliding windows m_n*. The linguistic variables used to represent them were divided into three levels: *low*, *moderate*, and *high*. The consequent – the possibility that an event occurs – was divided into five levels,*very strong*, *strong* , *medium* , *weak* and *very weak*. We used trapezoidal membership functions (MFs) to represent *low, high, very strong, very weak*; and triangle MFs to represent *moderate, medium , strong, weak*. We show these MFs in Figure 4.3(a) and 4.3(b).

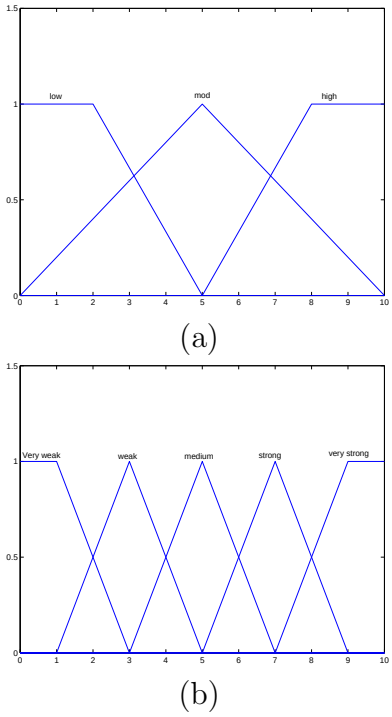

Figure 4.3. MFs used to represent the linguistic labels.

Based on the fact that when event occurs, E_s or m_n should be high. We design a fuzzy logic system using rules such as:

R^l : IF E_s is F_1^l and m_n is F_2^l, THEN the possibility that there is event (y) is G^l.

where $l = 1, \cdots, 9$. We summarize all the rules in Table 4.1.

4.4 Simulations

Figure 4.4 shows the basic data set, which was collected from Berkeley MICA2 motes, we used in our simulations. In order to get the probability of detection $P - d$, and probability of false alarm $P - f$, white Gaussian Noise is added, Signal-to-Noise Ratio (SNR) is $10dB$. We ran 100,000 Monte-Carlo simulations. The results of each algorithms are summarized in Table 4.2. Obviously, in terms of both P_d and P_f, the performances of both Double Sliding Window scheme and hybrid event-detection algorithm based on

Table 4.1. Rules for event-detection. Antecedent 1 is E_s, Antecedent 2 is m_n.

Rule	Antecedent 1	Antecedent 2	Consequent
1	low	low	very weak
2	low	mod	weak
3	low	high	mod
4	mod	low	weak
5	mod	mod	mod
6	mod	high	strong
7	high	low	mod
8	high	mod	strong
9	high	high	very strong

FLS are much better than that of signal strength event-detection algorithm.

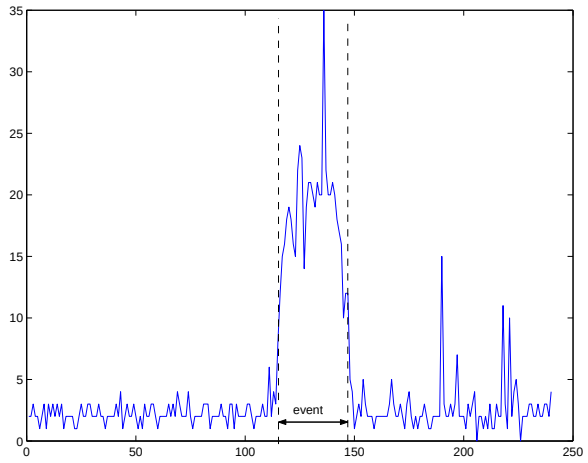

Figure 4.4. 240 sensed data set, the sample period is 1024ms.

4.5 Chapter Summary

In this chapter, we proposed two event-detection algorithms in Wireless Sensor Networks, Double Sliding Window scheme and hybrid approach based on Fuzzy Logic System. We use the basic data set collected by MOTE-Kit[35] test-bed and white Gaussian Noise is

Table 4.2. Probabilities of detection and false alarms .

	P_d	P_f
Signal Strength event-detection	69.75%	0.08%
Double Sliding Window event-detection	91.499%	0.02%
Hybrid event-detection based on FLS	99.97%	0.05%

added. Simulation results show that both the Double Sliding Window and the hybrid scheme based on FLS outperform the existing Signal Strength event-detection algorithm in terms of both the probability of detection and the probability of false alarm.

CHAPTER 5

EVENT FORECASTING FOR WIRELESS SENSOR NETWORKS

This chapter proposes using fuzzy logic system to forecast the events in wireless sensor networks. Section 5.1 will first study the self-similarity property of the sensed data in wireless sensor network, which means that the sensed data are forecastable. Type-2 Fuzzy Set and Interval Type-2 Fuzzy Logic Systems will be introduce in Section 5.2. We proposed to forecast the sensed signal strength and event using interval Type-2 fuzzy logic system in Section 5.3 and Section 5.4 respectively. The simulation result is shown in Section 5.5. Section 5.6 gives a summary of this chapter.

5.1 Self-Similarity of Sensed Signal Strength in wireless sensor network

For a detailed discussion on self-similarity in time-series, see [82, 98]. Here we briefly present its definition [16]. Given a zero-mean, stationary time-series $X = (X_t; t = 1, 2, 3, \cdots)$, we define the m-aggregated series $X^{(m)} = (X_k^{(m)}; k = 1, 2, 3, \cdots)$ by summing the original series X over nonoverlapping blocks of size m. Then it's said that X is H-self-similar, if, for all positive m, $X^{(m)}$ has the same distribution as X rescaled by m^H. That is,

$$X_t \equiv m^{-H} \sum_{i=(t-1)m+1}^{tm} X_i \quad \forall m \in N. \tag{5.1}$$

If X is H-self-similar, it has the same autocorrelation function $r(k) = E[(X_t - \mu)(X_{t+k} - \mu)]/\sigma^2$ as the series $X^{(m)}$ for all m, which means that the series is distributively self-similar: the distribution of the aggregated series is the same as that of the original.

Self-similar processes can show *long-range dependence*. A process with long-range dependence has an autocorrelation function $r(k) \sim k^{-\beta}$ as $k \to \infty$, where $0 < \beta < 1$. The degree of self-similarity can be expressed using *Hurst* parameter $H = 1 - \beta/2$. For self-similar series with long-range dependence, $1/2 < H < 1$. As $H \to 1$, the degree of both self-similarity and long-range dependence increases.

One method that has been widely used to verify self-similarity is the *variance-time plot*, which relies on the slowly decaying variance of a self-similar series. The variance of $X^{(m)}$ is plotted against m on a log-log plot, and a straight line with slope $(-\beta)$ greater than -1 is indicative of self-similarity, and the parameter H is given by $H = 1 - \beta/2$. We use this method to verify the self-similarity of acoustic signal.

In our experiments, 8 sensors were deployed in a lab. The location of each sensor is plotted in Fig. 5.1. We designed two scenarios, one is with a fixed source, and the other is without a fixed source. In Fig. 5.2, we plot the variance of $X^{(m)}$ against m on a log-log plot for 8 sensor node data respectively in the first scenario and Fig. 5.3 is under the second scenario. From the two figures, it's very clear that the no matter under what kind of condition the sensor network data have self-similarity because their traces have slopes much greater than -1.

5.2 Introduction Interval Type-2 Fuzzy Logic Systems

5.2.1 Introduction to Type-2 Fuzzy Set

The concept of type-2 fuzzy sets was introduced by Zadeh [106] as an extension of the concept of an ordinary fuzzy set, *i.e.*, a type-1 fuzzy set. Type-2 fuzzy sets have grades of membership that are themselves fuzzy [19]. A type-2 membership grade can be any subset in $[0, 1]$ – the *primary membership*; and, corresponding to each primary membership, there is a *secondary membership* (which can also be in $[0, 1]$) that defines the possibilities

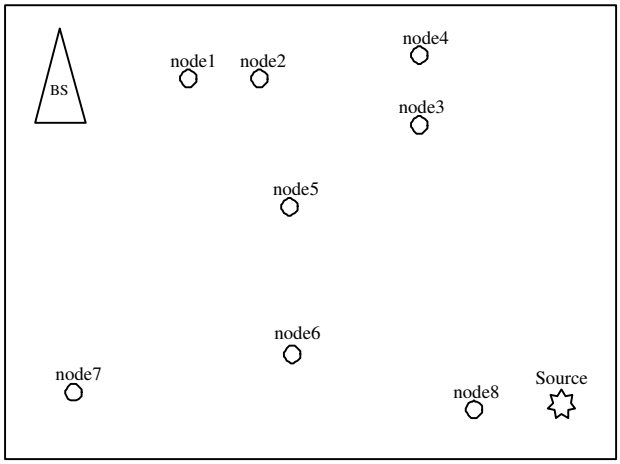

Figure 5.1. The deployment of eight sensor nodes in our experiments.

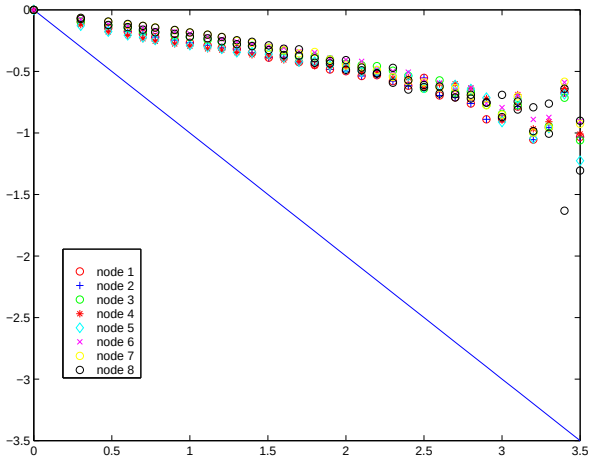

Figure 5.2. The *variance-time* plot (fixed source).

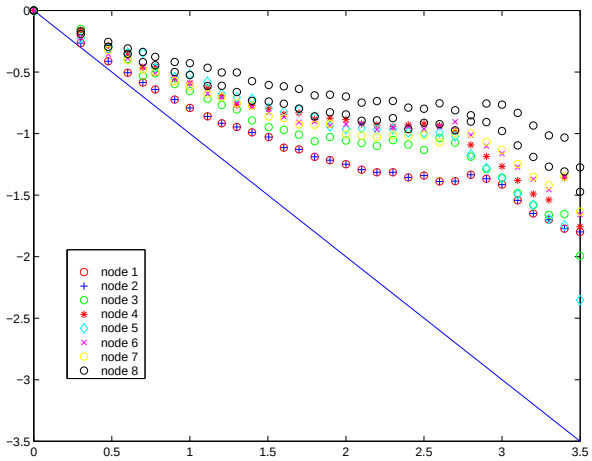

Figure 5.3. The *variance-time* plot .

for the primary membership. A type-1 fuzzy set is a special case of a type-2 fuzzy set; its secondary membership function is a subset with only one element, unity. Type-2 fuzzy sets allow us to handle linguistic uncertainties, as typified by the adage "words can mean different things to different people." A fuzzy relation of higher type (e.g., type-2) has been regarded as one way to increase the fuzziness of a relation, and, according to Hisdal, "increased fuzziness in a description means increased ability to handle inexact information in a logically correct manner [36]".

Figure 5.4 shows an example of a type-2 set. The domain of the membership grade corresponding to $x = 4$ is also shown. The membership grade for every point is a Gaussian type-1 set contained in $[0, 1]$, we call such a set a "Gaussian type-2 set". When the membership grade for every point is a crisp set, the domain of which is an interval contained in $[0, 1]$, we call such type-2 sets "interval type-2 sets" and their membership grades "interval type-1 sets". Interval type-2 sets are very useful when we have no other knowledge about secondary memberships. An interval type-2 MF is characterized by an upper and lower MF [57]. An upper MF and a lower MF are two type-1 MFs which are bounds for the footprint of uncertainty of an interval type-2 MF. The upper MF is a subset which has the maximum membership grade of the footprint of uncertainty; and, the lower MF is a subset which has the minimum membership grade of the footprint of uncertainty.

Example 1: Gaussian Primary MF with Uncertain Mean

Consider the case of a Gaussian primary MF having a fixed standard deviation, σ_k^l, and an uncertain mean that takes on values in $[m_{k1}^l, m_{k2}^l]$, i.e.,

$$\mu_k^l(x_k) = \exp\left[-\frac{1}{2}(\frac{x_k - m_k^l}{\sigma_k^l})^2\right], \quad m_k^l \in [m_{k1}^l, m_{k2}^l] \tag{5.2}$$

where: $k = 1, \ldots, p$; p is the number of antecedents; $l = 1, \ldots, M$; and, M is the number of rules. The upper MF, $\overline{\mu}_k^l(x_k)$, is (see Fig. 5.5)

$$\overline{\mu}_k^l(x_k) = \begin{cases} \mathcal{N}(m_{k1}^l, \sigma_k^l; x_k)\,, & x_k < m_{k1}^l \\ 1\,, & m_{k1}^l \le x_k \le m_{k2}^l \\ \mathcal{N}(m_{k2}^l, \sigma_k^l; x_k)\,, & x_k > m_{k2}^l \end{cases} \tag{5.3}$$

where, for example, $\mathcal{N}(m_{k1}^l, \sigma_k^l; x_k) \triangleq \exp\left(-\frac{1}{2}(\frac{x_k - m_{k1}^l}{\sigma_k^l})^2\right)$.

The lower MF, $\underline{\mu}_k^l(x_k)$, is (see Fig. 5.5)

$$\underline{\mu}_k^l(x_k) = \begin{cases} \mathcal{N}(m_{k2}^l, \sigma_k^l; x_k)\,, & x_k \le \frac{m_{k1}^l + m_{k2}^l}{2} \\ \mathcal{N}(m_{k1}^l, \sigma_k^l; x_k)\,, & x_k > \frac{m_{k1}^l + m_{k2}^l}{2} \end{cases} \tag{5.4}$$

□

5.2.2 Introduction to Type-2 FLS

Figure 5.6 shows the structure of a type-2 FLS[52]. It is very similar to the structure of a type-1 FLS [61]. For a type-1 FLS, the *output processing* block only contains the defuzzifier. We assume that the reader is familiar with type-1 FLSs, so that here we focus only on the similarities and differences between the two FLSs.

The fuzzifier maps the crisp input into a fuzzy set. This fuzzy set can, in general, be a type-2 set. In the type-1 case, we generally have "IF-THEN" rules, where the lth rule has the form

"R^l : *IF* x_1 *is* F_1^l *and* x_2 *is* F_2^l *and* $\cdots$ *and* x_p *is* F_p^l, *THEN* y *is* G^l",

where: x_is are inputs; F_i^ls are antecedent sets ($i = 1, \ldots, p$); y is the output; and G^ls are consequent sets. The distinction between type-1 and type-2 is associated with the nature of the membership functions, which is not important while forming rules; hence, the structure of the rules remains exactly the same in the type-2 case, the only difference being that now some or all of the sets involved are of type-2; so, the lth rule in a type-2 FLS has the form

"R^l : *IF* x_1 *is* $\tilde{F}_1^l$ *and* x_2 *is* $\tilde{F}_2^l$ *and* $\cdots$ *and* x_p *is* $\tilde{F}_p^l$, *THEN* y *is* $\tilde{G}^l$".

In the type-2 case, the inference process is very similar to that in type-1. The inference engine combines rules and gives a mapping from input type-2 fuzzy sets to output type-2 fuzzy sets. To do this, one needs to find unions and intersections of type-2 sets, as well as compositions of type-2 relations.

In a type-1 FLS, the defuzzifier produces a crisp output from the fuzzy set that is the output of the inference engine, *i.e.*, a type-0 (crisp) output is obtained from a type-1 set. In the type-2 case, the output of the inference engine is a type-2 set; so, "extended versions" (using Zadeh's Extension Principle [106]) of type-1 defuzzification methods were proposed in[52]. The type-reduction gives a type-1 fuzzy set called "type-reduction set".

To obtain a crisp output from a type-2 FLS, we can defuzzify the type-reduced set. The most natural way of doing this seems to be by finding the centroid of the type-reduced set; however, there exist other possibilities like choosing the highest membership point in the type-reduced set.

General type-2 FLSs are computationally intensive, because type-reduction is very intensive. Things simplify a lot when secondary membership functions (MFs) are interval

sets (in this case, the secondary memberships are either 0 or 1). When the secondary MFs are interval sets, the type-2 FLSs are called "interval type-2 FLSs". In [57], Liang and Mendel proposed the theory and design of interval type-2 FLSs. They proposed an efficient and simplified method to compute the input and antecedent operations for interval type-2 FLSs, one that is based on a general inference formula for them.

In an interval type-2 nonsingleton FLS with type-2 fuzzification and meet under minimum or product t-norm, the result of the input and antecedent operations, F^l, is an interval type-1 set, i.e., $F^l = [\underline{f}^l, \overline{f}^l]$, where $\underline{f}^l$ and $\overline{f}^l$ simplify to

$$\underline{f}^l = \underline{\mu}_{\tilde{\mathrm{F}}_1^l}(x_1) \star \ldots \star \underline{\mu}_{\tilde{\mathrm{F}}_p^l}(x_p) \tag{5.5}$$

and

$$\overline{f}^l = \overline{\mu}_{\tilde{\mathrm{F}}_1^l}(x_1) \star \ldots \star \overline{\mu}_{\tilde{\mathrm{F}}_p^l}(x_p) \tag{5.6}$$

where x_i $(i = 1, \ldots, p)$ denotes the location of the singleton. In this paper, we use center-of-sets type-reduction [57], which can be expressed as:

$$Y_{\cos}(Y^1, \cdots, Y^M, F^1, \cdots, F^M) = [y_l, y_r] = \int_{y^1} \cdots \int_{y^M} \int_{f^1} \cdots \int_{f^M} 1 \Big/ \frac{\sum_{i=1}^{M} f^i y^i}{\sum_{i=1}^{M} f^i} \tag{5.7}$$

where $Y_{\cos}$ is an interval set determined by two end points, y_l and y_r; $f^i \in F^i = [\underline{f}^i, \overline{f}^i]$; $y^i \in Y^i = [y_l^i, y_r^i]$, and Y^i is the centroid of the type-2 interval consequent set $\tilde{\mathrm{G}}^i$, and, $i = 1, \ldots, M$. We also use the training method proposed in [57] for designing an interval type-2 FLS in which its parameters are tuned.

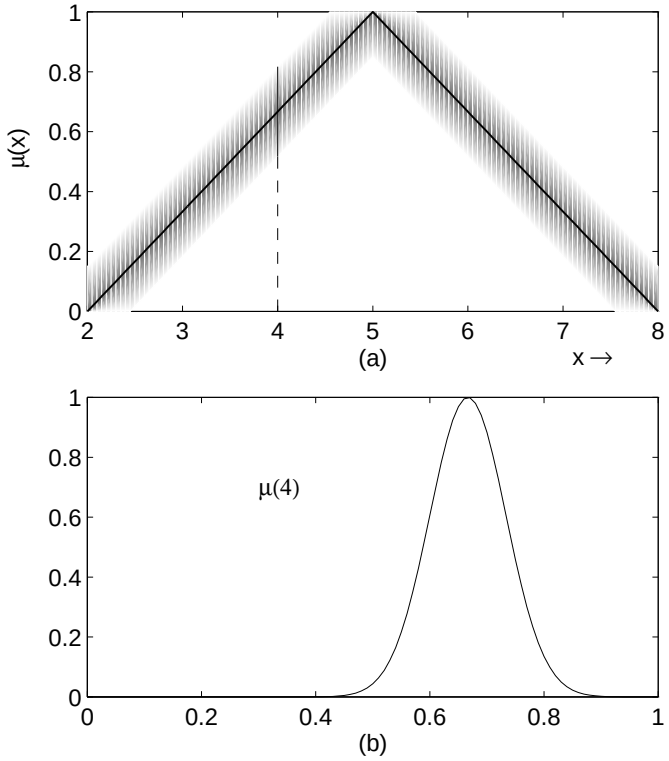

Figure 5.4. Representation of a Gaussian type-2 set.

5.3 Sensed Signal Strength Forecasting Using Interval Type-2 FLS

Acoustic amplitude sensor node measures sound amplitude at its microphone. Assuming that the sound source is a point source and sound propagation is lossless and isotropic, a root-mean-squared (RMS) amplitude measurement z is related to the sound source position X as

$$z = \frac{a}{\|X - \varsigma\|} + w, \tag{5.8}$$

where a is the RMS amplitude of the sound source, ς is the location of the sensor, and w is RMS measurement noise [53]. According to [53], w is modeled as a Gaussian with zero mean and variance σ^2. The sound source amplitude a is also modeled as a random quantity, which is uniformly distributed in the interval $[a_{lo}, a_{hi}]$. Given the location of the sound source X and the sensor position ς, $\frac{a}{\|X-\varsigma\|}$ is uniformly distributed as a is.

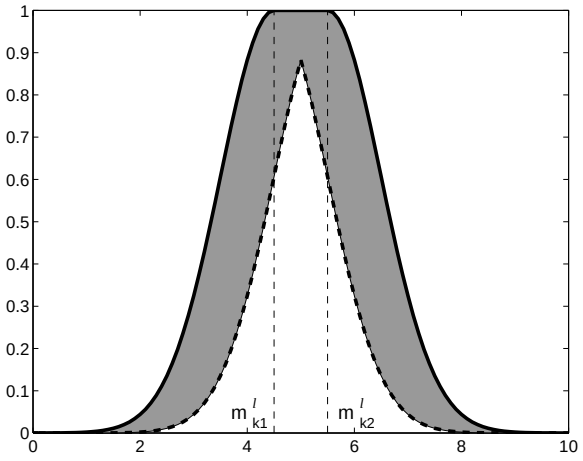

Figure 5.5. The interval type-2 MFs with fixed std and uncertain mean.

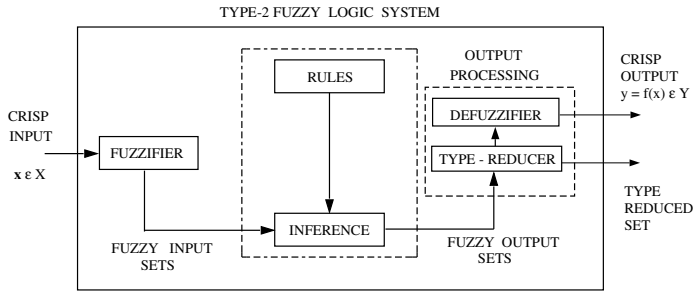

Figure 5.6. The structure of a type-2 FLS.

Therefore, z should be modeled as a Gaussian primary MF having a fixed standard deviation and an uncertain mean, as shown in Fig 5.5.

FLSs have been extensively used in time-series forecasting (e.g., [62, 57]). Since the sensed signal strength in wireless sensor network is self-similar as demonstrated in Section 5.1, its characteristics can be captured, which also means it can be forecasted. Here we apply an interval Type-2 FLS to do a multi-step forecasting, the step size is L. We use four antecedents, *i.e.*, $x(k-4\times L)$, $x(k-3\times L)$, $x(k-2\times L)$, and $x(k-1\times L)$, as inputs of the FLS to predict $x(k)$. Similarly, we use $x(k-4\times L+i)$, $x(k-3\times L+i)$, $x(k-2\times L+i)$, and $x(k-1\times L+i)$ to predict $x(k+i)$, $\forall i < L$. If antecedent has two fuzzy sets, the number of rules is $2^4 = 16$. The rules are set up as one example shown

bellow:

$$R^l : \text{IF } x(k-4\times L) \text{ is } \tilde{\text{F}}_1^l \text{ and } x(k-3\times L) \text{ is } \tilde{\text{F}}_2^l \text{ and } x(k-2\times L) \text{ is } \tilde{\text{F}}_1^l \text{ and } x(k-1\times L) \text{ is } \tilde{\text{F}}_2^l, \text{ THEN } x(k) \text{ is } \tilde{G}^l.$$

We use center-of-sets type reduction and steepest descent training algorithm [57] to design this interval type-2 FLS.

For comparison, we also design a type-1 FLS for signal strength forecasting. Antecedents are the same as in the interval type-2 FLS, however Gaussian MFs are chosen for this type-1 FLS. There are also 16 rules, since each of the antecedents has 2 fuzzy sub-set as well. The rule is designed as:

$$R^l : \text{IF } x(k-4\times L) \text{ is } \text{F}_1^l \text{ and } x(k-3\times L) \text{ is } \text{F}_2^l \text{ and } x(k-2\times L) \text{ is } \text{F}_1^l \text{ and } x(k-1\times L) \text{ is } \text{F}_2^l, \text{ THEN } x(k) \text{ is } G^l.$$

We use center-of-sets defuzzifier and steepest descent training algorithm to design this type-1 FLS.

5.4 Event Forecasting

Our event forecasting scheme consists of two steps:

1. Sensed signal strength forecasting, which has already been explained in the previous section;

2. Event detection. Double sliding window event detection scheme, which was proposed in the previous section is used here.

The double sliding window event-detection algorithm calculates two consecutive sliding windows of the sensed signal energy. The basic principle is to form the decision variable as the ratio of the total energy contained inside the two windows. Figure 4.1 shows the windows A and B and the response of the ratio m_n to the start and end of a sensed event. It can be seen that when only noise is sensed the response is flat, since both windows contain ideally the same amount of noise energy. The calculation of the window A and window B value is represented as in (4.4) to (4.6).

The advantages of this approach are:

- The decision variable m_n does not depend on the sensed signal energy, but on the ratio of the energy of two consecutive windows;

- Not only can we predict the starting edge of the event, but also the ending edge, *i.e.* , when M_n below the threshold Th_2, the event is claim ending(see Fig. 4.1.(b)).

5.5 Simulations

Our simulations were based on $N = 480$ samples, $x(1)$, $x(2)$, ..., $x(480)$. The first 240 data, $x(1)$, $x(2)$, ..., $x(240)$, are for training, and the remaining 240 data, $x(241), x(242)$, $\ldots, x(480)$ are for testing. In Fig. 5.7, we plot the sensed data that we used for training and testing, $x(1)$, $x(2)$, ..., $x(480)$. A standard $1kHz$ audio signal with different volume levels was used to simulate the events. Each sample has $1024ms$ duration.

We applied a type-1 FLS and an interval type-2 FLS for sensed signal forecasting. The initial locations of antecedent MFs were based on the mean, m_t, and std, σ_t, of the training data set. The parameters and number of parameters in the type-1 FLS and interval type-2 FLS are summarized in Table 5.1. The initial values we choose for the

Gaussian MFs are listed in Table 5.2. Then, we use steepest descent algorithm to train all the parameters based on the training data. After training, all the parameters and rules are fixed and we test the interval type-2 FLS based on the remaining 240 samples, $x(241)$, $x(242)$, ..., $x(480)$. We set the step size as $L = 5$ in both the type-1 FLS and the interval type-2 FLS. Meanwhile, the window size M equals to 5 in double sliding window event-detection as well. That makes the sensed signal forecasting meaningful.

Table 5.1. The parameters in type-1 and interval type-2 FLSs

FLS	type-1	interval type-2
Parameters in one antecedent	$m_{\mathrm{F}_k^i}$, $\sigma_{\mathrm{F}_k^i}$	$m_{\tilde{\mathrm{F}}_{k1}^i}$, $m_{\tilde{\mathrm{F}}_{k2}^i}$, $\sigma_{\tilde{\mathrm{F}}_k^i}$
Parameters in one consequent	$\overline{y}^i$	y_l^i, y_r^i
Total number of Parameters	144	224

Table 5.2. Initial values of the parameters in type-1 and interval type-2 FLSs

	Type-1 FLS	Interval Type-2 FLS
mean	$m_t - 2\sigma_t$ or $m_t + 2\sigma_t$	$[m_t - 2.5\sigma_t, m_t - 1.5\sigma_t]$ or $[m_t + 1.5\sigma_t, m_t + 2.5\sigma_t]$
σ	$\sigma_{\mathrm{F}_k^i} = 2\sigma_t$	$\sigma_{\tilde{\mathrm{F}}_k^i} = 2\sigma_t$
consequent	$\overline{y}^i \in [min, max]$	$y_l^i = \overline{y}^i - \sigma_t$, $y_r^i = \overline{y}^i + \sigma_t$

We compared the performance of the interval type-2 FLS with that of the type-1 FLS for sensed signal strength forecasting. For each FLS, we ran 100 Monte-Carlo realizations to eliminate the randomness of the consequences, and the two FLSs were tuned using a simple steepest-descent algorithm for 5 epochs. We used the testing data to see how each FLS performed by evaluating the root-mean-square-error (RMSE) between the de-

fuzzified output of the FLS and the actual sensor data ($x(k+1)$), *i.e.*,

$$\text{RMSE} = \sqrt{\frac{1}{240}\sum_{k=241}^{480}[x(k) - f(\mathbf{x}^k)]^2}, \tag{5.9}$$

where $\mathbf{x}^k = [x(k-4\times5), x(k-3\times5), x(k-2\times5), x(k-1\times5)]^T$, and T denotes transpose. The RMSE of all simulations are summarized in Figure 5.8. Observe Figure 5.8, the interval type-2 FLS outperforms the type-1 FLS in the sensed signal strength forecasting.

We are more interested in the system's capability of forecasting the events, especially the starting point of the events. We used the forecasted data sets to detect the starting point of the events, *i.e.*, the time stamp of event occurrence and then compared with the actual time stamp. We evaluated our double sliding window algorithm and compared it against the cumulated signal strength scheme[60]. We chose $Th_1 = mean + std$ for the double sliding window event detection. Since the threshold is hard to choose for cumulated signal strength scheme, we ran simulation for 3 different thresholds: *i.e.*, $mean$, $mean + std/2$ and $mean + std$. We also ran 100 Monte-Carlo simulations so as to get the average absolute error between the forecasted and actual time stamp, $\frac{1}{100}\sum_{i=1}^{100}|D_i - P_i|$, where D_i is the detected starting point (based on the forecasted signal) and P_i is the actual starting point. The results are summarized in Table 5.3.

Observe Table 5.3, the performance of event detection based on the forecasted signal from type-2 FLS is much better than that based on the forecasted signal from type-1 FLS. Meanwhile, our double sliding window is more effective than the existing cumulated signal strength scheme. Event forecasting helps us for power on/off management of the wireless sensor network, *i.e.* , we can power on the communication part of sensor nodes only when event has been forecasted. Since the sensor, signal processing parts consume less than 1/10 of the energy consumed by the communication part[89], this power on-off

strategy can save the energy tremendously.

Table 5.3. Average absolute error between the forecasted and actual time stamp

	type-1 FLS	interval type-2 FLS
double sliding window	7.8	1.4
SS with $th = m$	57.8	18.7
SS with $th = m + \sigma/2$	24.4	13.0
SS with $th = m + \sigma$	20.5	16.6

5.6 Chapter Summary

In this chapter, we proposed an event forecasting scheme for wireless sensor networks using interval type-2 fuzzy logic system. Our event forecasting scheme consists of two steps: sensed signal strength forecasting and event detection. We demonstrated that real-world sensed acoustic signals are self-similar, which means they are forecastable. We showed that a type-2 fuzzy membership function (MF), *i.e.*, a Gaussian MF with uncertain mean is appropriate to model the sensed signal strength of wireless sensors. We then applied an interval type-2 FLS to perform sensed signal forecasting. Furthermore, we proposed a double sliding window for event detection based on the forecasted signal, and compared it against the existing cumulated signal strength scheme. Simulation results show that FLSs can be used for sensed signal strength forecasting, and the interval type-2 FLS performs much better than the type-1 FLS in sensed signal forecasting. The sensed signal forecasting can further be used for event detection, and the average absolute error between the actual starting point and the point detected based on the sensed signal from the interval type-2 FLS is much smaller than the one based on the sensed signal from the type-2 FLS.

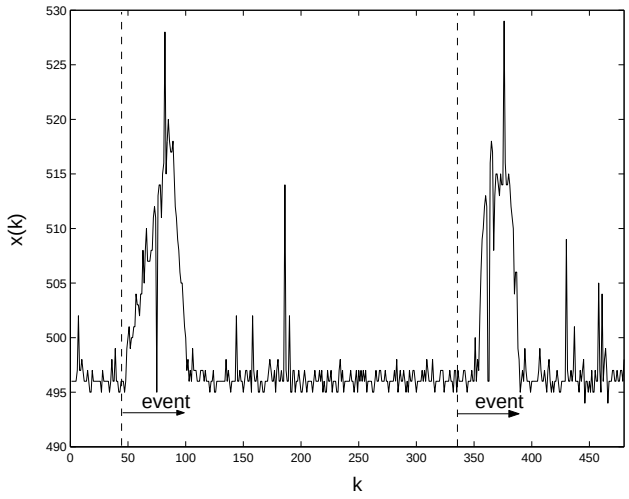

Figure 5.7. Sensed data for 1024 seconds. (The sample period is 1024ms).

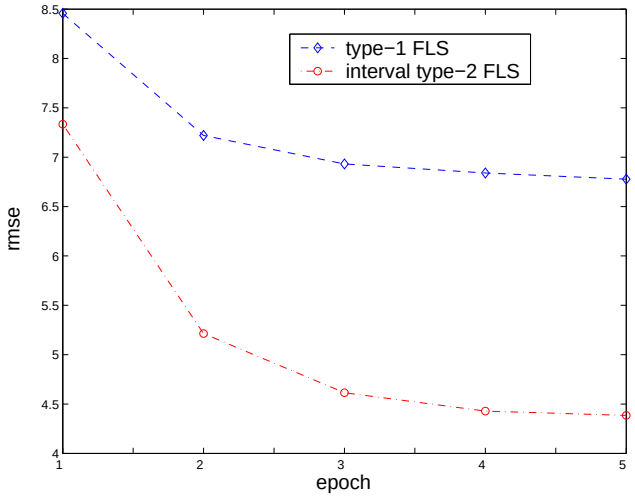

Figure 5.8. The forecasting RMSE by two FLSs.

CHAPTER 6

REDUNDANCY REDUCTION IN WIRELESS SENSOR NETWORKS

6.1 Cross-similarity of Sensor Network Data

Usually, in wireless sensor networks, sensor nodes are densely deployed, *e.g.*, tens of sensor nodes per square meters [63], therefore the information data collected from adjacent sensor nodes might be very similar with each other, that also means there exists redundancy among those information.

The study about self-similarity in Section 5.1 can be extended. We try to prove that not only does the data from one sensor node have self-similarity, but cross-similarity among the data of all the adjacent sensor nodes have cross-similarity as well, which can directly demonstrate that there exists redundancy in the collected data of the wireless sensor networks. In order to prove that, we mixed the data sets together to get a new time series as $Y = (X_t^1, X_t^2, \cdots, X_t^8; t = 1, 2, 3, \cdots)$. We test its self-similarity by plotting the variance-time curve in Fig 6.1 as well. From these three figures, it's very clear that the no matter under what kind of condition both the single sensor network data and the mixed sensor networks data have self-similarity because their traces have slopes much greater than -1.

6.2 Redundancy Reduction in Wireless Sensor Networks Using SVD-QR

In the previous section, we have proved that the data sets collected by adjacent sensor nodes are quite similar with each other. It is clear that there exists redundancy among the collected information. Therefore, two questions are popping up. Is such kind of redundancy profitable? Does more copies of the data set mean better estimates? The answers

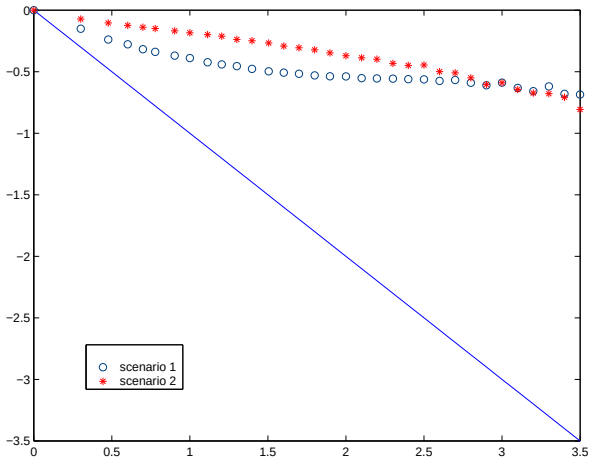

Figure 6.1. The *variance-time* plot for mixed sensor data.

are both no. The goal of wireless sensor networks is to monitor the physical world, provide enough information in which users are interested so that users can perform further tasks, *e.g.*, events detection, targets estimating and tracking. Blair and Bar-Shalom have already demonstrated in [9] that more data from more sensor nodes doesn't mean better performance in terms of the maximum root-mean square errors(RMSE). Meanwhile, if we can get enough information from less sensor nodes, we can turn off the other sensor nodes so as to preserve energy and prolong the lifetime of the whole networks.

How to select the principal nodes to effectively represent the whole neighborhood? We view the data from all the adjacent sensor nodes as a matrix P, each column of P is the data from one sensor node, each row of P is the data collected at one epoch from all the sensor nodes. Therefore, the principal nodes picking problem can be simplified as subset selection.

Several subset selection methods exist [14], but a singular value decomposition (SVD) method is preferable in rank deficient problems [26]. Furthermore, the SVD provides a natural way to separate a space into dominant and subdominant subspaces. If we view the data matrix P as a span of the input subspace, then the SVD decomposes the span

into an equivalent orthogonal span, from which we can identify the dominant and sub-dominant spans. In this way, we solve two problems simultaneously: (i) we estimate the data sets from *how many* sensor nodes are needed to effectively represent the neighborhood, and, (ii) we identify the data sets from *which* sensor nodes are the principal ones. The remainder can be discarded, and those sensor nodes can be turned off to conserve the energy.

6.2.1 Introduction of SVD-QR Algorithm

Here, we use the following SVD-QR algorithm that is similar to the one in [26] and [27] to select a set of independent data sets that minimize the residual error in a least-squares sense:

1. Given $P \in R^{N \times M}$, assume $N > M$, and $rank(P) = r \leq M$ denote the rank of P. Determine a numerical estimate $r^{'}$ of the rank of the data sets matrix P by calculating the singular value decomposition

$$P = U \begin{bmatrix} \Sigma & 0 \\ 0 & 0 \end{bmatrix} V^T, \tag{6.1}$$

   where, U is an $N \times N$ matrix of orthonormalized eigenvectors of PP^T, V is an $M \times M$ matrix of orthonormalized eigenvectors of P^TP , and Σ is the diagonal matrix $\Sigma = diag(\sigma_1, \sigma_2, \ldots, \sigma_r)$, where σ_i denotes the i^{th} singular value of P, and $\sigma_1 \geq \sigma_2 \geq \cdots \geq \sigma_r > 0$. Select $\hat{r} \leq r^{'}$.

2. Calculate a permutation matrix Π such that the columns of the matrix $\Gamma_1 \in R^{N \times \hat{r}}$ in

$$P\Pi = [\Gamma_1, \Gamma_2] \tag{6.2}$$

are independent. The permutation matrix Π is obtained from the QR decomposition of the sub-matrix comprised of the right singular vectors, which correspond to the $\hat{r}$ ordered *most-significant* singular values.

In short, we select the data sets as the following:

- Decomposes P, from the SVD of P, save V.

- Observe Σ. Select an appropriate $\hat{r}$.

- Partition

$$V = \begin{bmatrix} V_{11} & V_{12} \\ V_{21} & V_{22} \end{bmatrix} \tag{6.3}$$

  where $V_{11} \in R^{\hat{r}\times\hat{r}}$, $V_{12} \in R^{\hat{r}\times(M-\hat{r})}$, $V_{21} \in R^{(M-\hat{r})\times\hat{r}}$, and $V_{22} \in R^{(M-\hat{r})\times(M-\hat{r})}$.
  In many practical cases, σ_1 is much larger than $\sigma_{r'}$; thus $\hat{r}$ can be chosen much smaller than the estimate $r^{'}$ of rank(P), even 1.

- Using QR decomposition with column pivoting, determine Π such that

$$Q^T[V_{11}^T, V_{21}^T]\Pi = [R_{11}, R_{12}], \tag{6.4}$$

  where Q is a unitary matrix, and R_{11} and R_{12} form an upper triangular matrix; and Π is the permutation matrix, the column permutation Π is chosen so that $abs(diag(R))$ is decreasing. In short, Π corresponds to the $\hat{r}$ ordered *most-significant* sets.

6.2.2 Examples of Redundancy Reduction Using SVD-QR

Here, we give an example of how to use SVD-QR decomposition to reduce the redundancy in wireless sensor networks, *i.e.*, determine *how many* sensors of data should be selected.

We use the data sets which also has been used in Section 5.1, and get one clip, *i.e.*, 8 sensor nodes, each one has 100 samples of data, as the input of the following example.

Example 2

- *step 1.* SVD the input matrix P, get:

  $diag(\Sigma) = (14160, 74, 20, 14, 13, 10, 9, 7)$;

  Clearly, $\Sigma(1,1)$ is much larger than $\Sigma(2,2)$. That means we can only select one data set to represent all the eight sets of data, *i.e.*, $\hat{r} = 1$.

- *step 2.* Partition the V, and get V_{11} and V_{21}, which are needed in QR decomposition, $V_{11} = -0.3565$, and

$$V_{21} = \begin{bmatrix} -0.3556 \\ -0.3535 \\ -0.3512 \\ -0.3546 \\ -0.3526 \\ -0.3540 \\ -0.3503 \end{bmatrix}.$$

- *step 3.* Using QR decomposition with column pivoting to determine the economy matrix Π. Since in this example, $\hat{r} = 1$, we only care about the first column of Π,

$$\Pi(:,1) = \begin{bmatrix} 1 \\ 0 \\ 0 \\ 0 \\ 0 \\ 0 \\ 0 \\ 0 \end{bmatrix}.$$

That means the first column of the input matrix P, *i.e.*, the data collected from the first sensor node is the *most-significant* one, which can effectively represent all the eight sensor nodes in the neighborhood. ♯

Example 3

What if we select more than one set of data? We have the following example to explain. We get another clip of data, still has 8 sensor nodes, each one has 100 samples of data, as the input.

- *step 1.* SVD the input matrix P, get:

  $diag(\Sigma) = (14759, 368, 275, 200, 186, 146, 97, 68)$.

  Oberserve Σ, the decreasing scope from $\Sigma(1,1)$ to $\Sigma(2,2)$ is not as large as it is in *Example 1* . So, we have $\hat{r} = 2$.

- *step 2.* Partition the V, and get V_{11} and V_{21},

$$V_{11} = \begin{bmatrix} -0.3503 & 0.1919 \\ -0.3582 & -0.1618 \end{bmatrix}, \text{ and}$$

$$V_{21} = \begin{bmatrix} -0.3528 & 0.3369 \\ -0.3570 & -0.8685 \\ -0.3580 & -0.1417 \\ -0.3525 & 0.0853 \\ -0.3585 & 0.1548 \\ -0.3406 & 0.1338 \end{bmatrix}.$$

- *step 3.* Using QR decomposition with column pivoting to determine the economy matrix Π. Since $\hat{r} = 2$, we only care about the two column of Π,

$$\Pi(:, 1:2) = \begin{bmatrix} 0 & 0 \\ 0 & 0 \\ 0 & 1 \\ 1 & 0 \\ 0 & 0 \\ 0 & 0 \\ 0 & 0 \\ 0 & 0 \end{bmatrix}.$$

  That means the forth and third columns of the input matrix P, *i.e.*, the data collected from the forth and third sensor nodes are the *most-significant* ones, which can effectively represent all the eight sensor nodes in the neighborhood. ♯

From our plenty of simulations, the significant one(s) are changing, that depends on the change of the environment. However, we can define a *coherent time* , in this time, the

environment is assumed to keep stable to a certain extend.

6.3 Chapter Summary

In this chapter, we first proved there exists not only self-similarity in the data from one sensor node, but cross-similarity among the data of all the adjacent sensor nodes also. That demonstrated that there exists redundancy in the collected data of the wireless sensor networks. Taking energy efficiency and better performance into consideration, we proposed to use SVD-QR to select the principal data sets from particular sensor nodes to represent the all the sensor nodes in the neighborhood effectively. We gave two examples to show how to do it.

CHAPTER 7

CONCLUSION

This chapter concludes the thesis. The chapter begins with a summary of the thesis results and contributions, follows with a discussion of future research directions in the physical layer design of wireless sensor networks.

7.1 Summary

This thesis has focused on the physical layer issues in the design of wireless sensor networks. The contributions of this thesis are:

MIMO Wireless Sensor Network: We discussed the virtual MIMO structure in wireless sensor network, set up MIMO system model focused on one-hop inter-cluster transmission. Investigated the error model of the channel estimation, and analyzed how the estimation error will impact the optimal water-filling strategy along with the numerical results based on the Monte-Carlo simulations [94, 95](chapter 2).

UWB Sensor Network: We proposed a hybrid TH/FH PPM UWB for wireless sensor networks, and based on this system we made a performance analysis with the presence of the multi-tone/pulse jammer interference and multi-user interference. An accurate expressions of SER and BER with the presence of MUI and hostile jammer interference was obtained. We also evaluated the performances for different selections of the parameters to show how these parameters affect to the system [96, 97](chapter 3).

Event Detection in Wireless sensor Networks: Two event detection schemes in Wireless Sensor Networks were proposed, including *double sliding window* and *hybrid hybrid event-detection using fuzzy logic system.* We collect the data set by MOTE-Kit[35] test-bed. Simulation results showed that both the *Double Sliding Window* and the *hybrid* scheme based on FLS outperform the existing Signal Strength event-detection algorithm in terms of both the probability of detection and the probability of false alarm [90](chapter 4).

Event Forecasting for Wireless Sensor Networks: An event forecasting scheme for wireless sensor networks using interval type-2 fuzzy logic system was proposed. We demonstrated that real-world sensed acoustic signals are self-similar, which means they are forecastable. A type-2 fuzzy membership function (MF), *i.e.*, a Gaussian MF with uncertain mean was shown to be appropriate to model the sensed signal strength of wireless sensors. The sensed signal forecasting can further be used for event detection, and the average absolute error between the actual starting point and the point detected based on the sensed signal from the interval type-2 FLS is much smaller than the one based on the sensed signal from the type-2 FLS [91, 92](chapter 5).

Redundancy reduction in wireless sensor networks: we first proved there exists not only self-similarity in the data from one sensor node, but cross-similarity among the data of all the adjacent sensor nodes also. That theocratically demonstrated that there exists redundancy in the collected data of the wireless sensor networks. Taking energy efficiency and better performance into consideration, we proposed to use SVD-QR to select the principal data sets from particular sensor nodes to represent the all the sensor nodes in the neighborhood effectively [93](chapter 6).

7.2 Future directions

7.2.1 Multiple Event Detection in wireless sensor networks

In our propose work in Chapter 4 and 5, we focused on single event detection in wireless sensor networks. However, it can be extended to a more meaningful multiple event detection and propagation problem, *i.e.*, the local sensing of a series of crucial events and the energy efficient data reporting the realization of these events to a (fixed or mobile) control center.

This work includes:

- The cooperation of local sensor nodes. Nearby sensor nodes work coordinately, make the detection for different events together so as to increase the probability of detection, P_d and decrease the probability of false alarm, P_f;

- Classification of multiple events. Events may belong to the same class, or not. E.g., in a battlefield, an event may mean the appearance of a soldier or a tank. If the sensor nodes can not only detect events, but also classify the events, it will a significant progress.

- Propagation through multiple hops. To reserve energy, the communication mode of WSN is multi-hop mode. After the local sensing, processing and detecting of the events, it is necessary to report the results to a control center, wherein a multi-hop transmission is a must. How to fuse all the data and achieve a reliable transmission is also important.

7.2.2 MIMO UWB for wireless sensor networks

The system we addressed in Chapter 3 is a Single Input Single Output (SISO) system. However, Multiple Input Multiple Output (MIMO) will be a better solution to wireless sensor networks. MIMO can achieve better performance in terms of error probability, i.e., BER, and high throughput [83]. The trade-off between diversity and multiplexing gains should be considered. Concerning the realization of MIMO, local nodes can be noncooperative, half-cooperative or cooperative. Energies consumed in transmission, processing circuitry and cooperation should be studied to get an optimal energy efficiency, satisfying diversity and multiplexing gains.

REFERENCES

[1] G. D. Abowd, and J. P. G. Sterbenz, "Final report on the interagency workshop on research issues for smart enviroments," *IEEE Personal Communications*, pp. 36-40, Octorber, 2000.

[2] J. Agre, and L. Clare, "An integrated architecture for cooperative sensing networks," *Computer*, vol. 33, Issure. 5, pp. 106-108, 2000.

[3] I. F. Akyildiz, W. Su, Y. Sankarasubramaniam, E. Cayirci, "Wireless sensor networks: a survey," *Computer Networks*, No. 38, pp. 393-422, 2002.

[4] S. M. Alamouti, "A simple transmit diversity techinique for wireless communications," *IEEE J. Sel. Areas. Commun.*, vol. 16, no. 8, pp. 1451-1458, Oct. 1998.

[5] http://www.alertsystem.org.

[6] M.D. Benedetto and G. Giancola, *Understanding Ultar Wide Band Radio Fundamentals*, Prentice Hall Technical Reference, NJ, USA, 2004

[7] M. Bengtsson, and B. Ottersten "Optimal and suboptimal transmit beamforming," in *Handbook of Antennas in Wireless Communications.*, L. C. Godara, Ed. Boca Raton, Fl: CRC, 2001.

[8] E. Biglieri, J. Proakis, and S. Shamai, "Fading channels: Information-theoretic and communication aspects," *IEEE Trans. Inf. Theory*, vol. 44, no. 6, pp. 2619-2692, Oct. 1998.

[9] W. D. Blair and Y. Bar-Shalom, "Tracking Maneuvering Targets with Multiple Sensors: Does More Data Always Mean Better Estimates?," *IEEE Trans. on Aerospace and Elec. Systems*, vol. 32, no. 1, pp. 450-455, Jan 1996.

[10] P. Bonnet, J. Gehrke, and P. Seshadri, "Querying the physical world," *IEEE Personal Communications*, pp. 10-15, October 2000.

[11] A. Cerpa, J. Elson, M. Hamilton, and J. Zhao, "Habitat monitoring: application driver for wireless communications technology," *ACM SIGCOMM'2000*, Costa Rica, April 2001.

[12] A. Chandrakasan, R. Amirtharajah, S. Cho, J. Coodman, G. Konduri, J. Kulik, W. Rahiner, and A. Wang, "Design considerations for distributed micro-sensor systems," *Proceedings of the IEEE 1999 Custom Integrated Circuits Conference*, pp. 279-286, San Diego, CA, May 1999.

[13] S. Chandrasekaran et al, " An eigenspace update algorithm for image analysis ," *Graphical Models and Image Processing*, Vol. 59, pp. 321-332, Sept. 1997.

[14] S. Chen, S. A. Billings, and W. Luo, "Orthogonal Least Squares Methods and their Application to Nonlinear System Identification," *Int. J. Control*, vol. 50, no. 5, pp. 1873-1896, 1989.

[15] A. G. Constantine, "Some non-central distribution problems in multivariate analysis," *Ann. Math. Stat.*, vol. 34, pp. 1270-1285, Dec. 1963.

[16] M. E. Crovella and A. Bestavros, "Self-similarity in world wide web traffic: evidence and possible causes," *IEEE Trans. on Networking*, vol. 5, no. 6, pp. 835-846, Dec 1997.

[17] S. Cui, A. J. Goldsmith, and A. Bahai, "Energy-efficiency of MIMO and cooperative MIMO techniques in sensor networks," *IEEE J. Sel. Areas. Commun.*, vol. 22, no. 6, pp. 1089-1098, Aug. 2004.

[18] P. F. Driessen, and G. J. Foschini, "On the capacity formula for multiple-input multiple-output wireless channels: A geometric interpretation ," *IEEE Trans. Commun.*, vol. 2, pp. 173-176, Feb. 1999.

[19] D. Dubois and H. Prade, *Fuzzy Sets and Systems: Theory and Applications*, Academic Press, New York, USA, 1980.

[20] I. A. Essa, "Ubiquitous sensing for smart and aware environments," *IEEE Personal Communications*, pp. 47-49, October, 2000.

[21] D. Estrin, R. Govindan, J. Heidemann, and S. Kumar,, " Next century chanlleges:scalable coordination in sensor networks ," *Mobicom 1999, Seattle, WA.*, pp. 263-270, August 1999.

[22] F. R. Farokhi, G. J. Foschini, A. Lozano, and R. A. Valenzuela, "Link-optimal space-time processing with multiple transmit and receiver antennas", *IEEE Commun. Lett.*, vol. 5, pp. 85-87, Mar. 2001.

[23] J. Foerster (editor), "Channel Modeling Sub-committee Report Final," IEEE802.15-02/490 (see http://ieee802.org/15/.

[24] A. Goldsmith, S. A. Jafar, N. Jindal, and S. Vishwanath, "Capacity limits of MIMO channels," *IEEE J. Sel. Areas. Commun.*, vol. 21, no. 5, pp. 684-702, June 2003.

[25] A. Goldsmith, and P. Varaiya "Capacity of fading channels with channel side information," *IEEE Trans. on Info. Theory.*, vol. 45, no. 5, pp. 1986-1992, Nov, 1997.

[26] G. H. Golub, and C. F. Van Loan, *Matrix Computations*, Johns Hopkins Univ. Press, MD 1983.

[27] G.H. Golub, "Numerical Methods for Solving Least Squares Problems," *Numer. Math*, no. 7, pp. 206-216, 1965.

[28] M. Gu and S. C. Eisenstat, " A stable and fast algorithm for updating the singular value decomposition ," Technical Report YALEU/DCS/RR-966, Yale University, New Haven, CT, 1994.

[29] P. Hall, D. Marshall and R. Martin " Incremental Eigenanalysis for Classification", *British Machine Vision Conference*, vol. 1, pp. 286-295, Sept. 1998.

[30] M. P. Hamilton, and M. Flaxman, "Scientific data visualization and biological diversity: new tools for spatializing multimedia observations of species and ecosystems," *Landscape and Urban Planning*, pp. 285-297, No. 21, 1992.

[31] M.V. Hegde, W.E. Stark and D. Teneketzis, "On the capacity of channels with unknown interference," *IEEE Transactions on Information Theory*, vol. 35, Issure. 4, pp. 770 - 783, July 1989.

[32] W. R. Heinzelman, J. Kulik, and H. Balakrishnan, " Adaptive protocols for infromation dissemination in wireless sensor networks", *Proceedings of the ACM MobiCom'99*, pp. 174-185, Seattle, Washinton, 1999.

[33] W. R. Heinzelman, A. chandrakasan, and H. Balakrishnan, " Energy-efficient communication protocol for wireless microsensor networks", *IEEE proceedings of the Hawaii International Conference on System Sciences*, pp. 1-10, Januray, 2000.

[34] C. Herring, and S. Kaplan, "Component-based software systems for smart environments," *IEEE Personal Communications*, pp. 60-61, October, 2000.

[35] J. L. Hill, and D. E. Culler, " Mica: A Wireless Platform for Deeply Embedded Networks ," *Micro, IEEE,*, Volume: 22, Issue: 6, pp. 12-24, Nov.-Dec. 2002.

[36] E. Hisdal, "The IF THEN ELSE statement and interval-valued fuzzy sets of higher type," *Int'l. J. Man-Machine Studies*, vol. 15, pp. 385-455, 1981.

[37] G. Hoblos, M. Straoswiecki, and A. Aitouche, "Optimal design of fault tolerant sensor networks," *Ieee International Conference on Control Applications*, pp. 467-472, Anchorage, Ak, Sepetember 2001.

[38] B. Hu, and N. C. Beaulieu, " Accurate Performance Evaluation of Time-Hopping and Direct-Sequence UWB Systems in Multi-User Interference ," *IEEE Transactions on Communications*, Volume: 53, No. 6, pp. 1053-1062, June. 2005.

[39] C. intanagonwiwat, R. Govindan, and D. Estrin, " Directed diffusion: a scalable and robust communication paradigm for sensor networks", *Proceedings of the ACM MobiCom'00*, pp. 56-67, Boston, MA, 2000.

[40] I. S. 802.11n, "Part 11: Wireless LAN mdeium access control (MAC) and physical layer (PHY) specifications - High throughput," *Working IEEE Standards*, 2006.

[41] I. S. 802.16e, "Part 16: Air interface for fixed and mobile broadband wireless access systems," *Working IEEE Standards*, Oct, 2005.

[42] I. S. 802.20, "Part 20: Mobile broadband wireless access (MBWA)," *Working IEEE Standards*, 2006.

[43] E. Jain, and Q. Liang, "Sensor placement and lifetime of wireless sensor networks: theory and performance analysis," *Sensor Network Operations*, edited by S. Phoha, T. F. La Porta, and C. Griffin, IEEE Press, Piscataway, NJ, 2004.

[44] W. C. Jakes Jr., *Mircowave Mobile Communications* New York: Wiley, 1974

[45] A. T. James, "Distributions of matric variates and latent roots derived from normal samples," *Ann. Math. Stat.*, vol. 35, pp. 475-501, June 1964.

[46] S. K. Jayaweera, and H. V. Poor, "MIMO Capacity results for Rician fading channels," *Proc. IEEE Global Telecommunications Conference*, vol. 4, pp. 1806-1810, Dec. 2003.

[47] S. K. Jayaweera, "Energy analysis of MIMO techniques in wireless sensor networks," *38th Annual Conf. on Inform. Sci. and Syst. (CISS 04)* Princeton, NJ, Mar. 2004

[48] S. K. Jayaweera, "An energy-efficient virtual MIMO communications architecture based on V-BLAST processing for distributed wireless sensor networks," *Proc. IEEE Secon.*, Santa Clara, CA, USA, Oct. 2004

[49] P. Johnson et al., "Remote continuous physiological monitoring in the home," *Journal of Telemed Telecare*, No. 2, vol. 2, pp. 107-113, 1996.

[50] J. M. Kahn, R. H. Katz, and K. S. J. Pister, "Next century challenges: mobile networking for smart dust," *Proceedings of the ACM MobiCom'99*, pp. 271-278, Washington, USA, 1999.

[51] R. Kannan and S.S Iyengar, "Game-theoretic models for reliable path-length and energy-constrained routing with data aggregation in wireless sensor networks ," *IEEE*

Journal on Selected Areas in Communications, vol. 22, Issure. 6, pp. 1141-1150, Aug 2004.

[52] N. N. Karnik, J. M. Mendel and Q. Liang, " Type-2 Fuzzy Logic Systems", *IEEE Trans. on Fuzzy Systems*, vol. 7, no. 6, Dec. 1999.

[53] L. E. Kinsler, A. R. Frey, A. B.Coppens and J. V. Sanders, *Fundamentals of Acoustic*, John Wiley and Sons, Inc., New York, USA, 1999.

[54] A. Levy and M. Lindenbaum " Sequential Karhunen-Loeve basis extraction and its application to images", *IEEE Trans. on image processing*, vol. 9, pp. 1371-1374, Aug. 2000.

[55] D. Li, K. Wong, Y. H. Hu, and A. Sayeed, "Detection, classification and tracking of targets in distributed sensor networks," *IEEE Signal Processing Magazine*, No. 19, Issue. 2, 2002.

[56] Q. Liang, L. Wang, and Q. Ren, "Fault-Tolerant and Energy Efficient Cross-Layer Design for Wireless Sensor Networks," *International Journal of Sensor Networks*, 2006.

[57] Q. Liang and J. M. Mendel, " Interval type-2 fuzzy logic systems: theory and design," *IEEE Trans. Fuzzy Systems.* vol. 8, no. 5, pp. 535-551, Oct 2000.

[58] V. Lottici, A. D. Andrea and U. Mengali, "Channel Estimation for Ultra-Wideband Communications," *IEEE Journal on Selected Areas in Communications*, vol. 20, No. 9, pp. 1638-1645, Dec 2002.

[59] E. H. Mamdani, " Applications of fuzzy logic to approximate reasoning using linguistic systems", *IEEE Trans. on Systems, Man, and Cybernetics*, vol. 26, no. 12, pp. 1182-1191, 1977.

[60] S. Meguerdichain, F. Koushanfar, G. Qu and M. Potkonjak, " Exposure in wireless ad-hoc sensor networks ," *Mobicom 2001*, Rome, Italy, July 2001.

[61] J. M. Mendel, "Fuzzy Logic Systems for Engineering : A Tutorial," *Proceedings of the IEEE*, vol. 83, no. 3, pp. 345-377, March 1995.

[62] J. M. Mendel and G. Mouzouris, " Designing fuzzy logic systems ," *IEEE Trans. Circuits and Systems – II: Analog and Digital Signal Processing*, vol. 44, no. 11, pp. 885-895, Nov 1997.

[63] R. Min, M. Bhardwaj, S. Cho, N. Ickes, E. Shin, A. Sinha, A. Wang, and A. Chandrakasan, "Energy-centric Enabling Technologies for Wireless Sensor Networks," *IEEE Wireless Coomun.*, vol. 9, pp. 28-39, Aug 2002.

[64] D. Nadig, and S. S. Iyengar, "Anew architecture for distributed sensor integration," *Proceedings of the IEEE Southeastcon'93*, Charlotte, NC, April 1993.

[65] S. Nanda, R. Walton, J. Ketchum, M. Wallace, and S. Howard, "A high-performance MIMO OFDM wireless LAN," *IEEE Communications Magazine*, Vol. 43, no. 2, pp. 101-109, Feb. 2005.

[66] N. Noury, T. Herve, V. Rialle, G. Virone, E. mercier G. Morey, A. Moro, and T. Porcheron, "Monitoring behavior in home using a small fall sensor," *IEEE-EMBS Special Topic Conference on Microtechnologies in Medicine and Biology*, pp. 607-610, October, 2000.

[67] A. Pascula-Iserte, D. P. Palomar, A. I. Perez-Neira, and M. A. Lagunas "A Robust maximin approach for MIMO communications with imperfect channel state information based on convex optimization," *IEEE. Trans. Singal Proc.*, vol. 54, no. 1, pp. 346-359, Jan. 2006.

[68] A. Paulraj, R. Nabra, and D. Gore, *Introduction to Space-Time Wireless Communicaitons*, Cambridge, UK: Cambridge University Press, 2003.

[69] E. M. Petriu, M. D. Georganas, D. C. Petriu, D. Makrakis, and V. Z. Groza, "Sensor-based information appliances," *IEEE Instrumentation and Measurement Magazine*, pp. 31-35, December, 2000.

[70] G. J. Pottie, and W. J. Kaiser, " Wireless integrated network sensors ," *Communications of the ACM*, vol. 43, no. 5, pp. 551-558, May 2000.

[71] J. Rabaey, J. Ammer, J. L. da Silva Jr., and D. Patel, "Pico-Radio: ad-hoc wireless networking of ubiquitous low-energy sensor/monitor nodes," *Proceedings of the IEEE Computer Society Annual Workshop on VLSI (WVLST'00)*, pp. 9-12, Orlando, Florida, April 2000.

[72] J. M. Rabaey, M. J. Ameer, J. L. da Silva Jr., D. Patel, and S. Roundy, "RicoRadio supports ad hoc ultra-low power wireless networking," *IEEE Computer Magazine*, pp. 42-48, 2000.

[73] T. S. Rappaport, *Wireless Communications* Englewood Cliffs, NJ: Prentice Hall, 1996

[74] R.C. Robertson and J.F. Sheltry, "Multiple tone interference of frequency-hopped noncoherent MFSK signals transmitted over Ricean fading channels," *IEEE Transactions on Communications*, vol. 44, Issure. 7, pp. 867 - 875, July 1996.

[75] A. A. M. Saleh and R. A. Valenzuela " A Statistical Model for Indoor Mulitpath Propagation", *IEEE Journal on Selected Areas in Communications*, vol. 5, no. 2, pp. 128-137, Feb. 1987.

[76] R. A. Scholtz, "Multiple Access with Time-Hopping Impulse Modulation," *IEEE Militray Communication Conference*, vol. 2, pp. 447-450, Oct 1993.

[77] C. Shen, C. srisathapornphat, and C. Jaikaeo, "Sensor information networking architecture and applications," *IEEE Personal Communications*, pp. 52-59, August, 2001.

[78] Z. Shen, R. W. Heath, Jr., J. G. Andrews, and B. L. Evans, "Comparison of Space-Time Water-filling and Spatial Water-filling for MIMO Fading Channels," *IEEE Global Telecommunications Conference, 2004*, Vol. 1, pp. 431-435, Dec, 2004. Dallas, TX.

[79] E. Shih, S. Cho, N. Ickes, R. Min, A. Sinha, A. Wang, and A. Chandrakasan, "Physical Layer Driven Protocol and Algorithm Design for Energy-Efficient Wireless Sensor Networks," *ACM International Conference on Mobile Computing and Networking*, pp: 272 - 287, Rome, Italy, 2001.

[80] B. Sibbald, "Use computerized systems to cut adverse drug events: report," *Canadian Medical Association Journal*, No. 164, vol. 13, p. 1878, 2001.

[81] K. Sohrabi, J. Gao, V. Ailawadhi, and G.J. Pottie, *Protocols for Self-Organization of a Wireless Sensor Network*, IEEE Personal Communications, October 2000.

[82] W. Stallings, *High-Speed Networks: TCP/IP and ATM Design Principles*, Upper Saddle River, NJ, 1998.

[83] V. Tarokh, A. Naguib, N. Seshadri and A. R.Calderbank, " Space-time codes for high data rate wireless communication: performance criteria in the presence of channel estimation errors, mobility, and multiple paths ," *IEEE Transactions on Communications*, Vol. 47, Issue 2, pp. 199-207, Feb. 1999

[84] I. E. Telatar, "Capacity of multi-antenna Gaussian channels", *Eur. Trans. Telecomm. ETT*, vol. 10, no. 6, pp. 585-596, Nov. 1999.

[85] D. Tse, and P. Viswanath, *Fundamentals of Wireless Communications* Cambridge, U.K.: Cambridge Univ. Press, 2005

[86] G.L. Turin, F.D. Clapp, T.L. Johnson, S.B. Fine and D. Lavy " A Statistical Model of Urban Multipath Propagation", *IEEE Trans. on Vehicular Technology*, vol. 21, pp. 1-9, Feb. 1972.

[87] M. Vipin, and M. El Zarki, "An ultra wide band (UWB) based sensor network for civil infrastructure health monitoring," *1st European Workshop on Wireless Sensor Networks (EWSN)*, Berlin, Germany, January 2004.

[88] M. Vu, and A. Paulraj, "MIMO wireless precoding," submitted to *IEEE Signal Processing Magazing.*, 2006.

[89] A. Y. Wang, and C. G. Sodini, " A Simple Energy Model for Wireless Microsensor Transceivers ," *Globecom 2004, Dallas, TX.*,

[90] Q. Liang, and L. Wang, " Event Detection in Sensor Networks Using Fuzzy Logic Systems," *IEEE Computational Intelligence for Homeland Security and Personal Safety*, March 2005, Orlando, Fl.

[91] Q. Liang, and L. Wang, " Event forecasting for wireless sensor networks using interval type-2 fuzzy logic systems," submitted to *Journal of Intelligent and Fuzzy systems.*

[92] Q. Liang, andL. Wang, " Sensed Signal Strength Forecasting for Wireless Sensors Using Interval Type-2 Fuzzy Logic System," *FUZZY-IEEE 2005*, May 2005, Reno, NV.

[93] Q. Liang, andL. Wang, " Redundancy Reduction in Wireless Sensor Networks Using SVD-QR," *IEEE Military Communication Conference*, , Oct. 2005, Atlantic City, NJ.

[94] L. Wang, and Q. Liang, " Channel Capacity with Imperfect Channel State Information at Low SNR in MIMO Wireless Sensor Networks," submitted to *WCNC 2006.*

[95] L. Wang, and Q. Liang, " Channel Capacity with Imperfect Channel State Information at Low SNR in MIMO Wireless Sensor Networks," to be submitted to IEEE Transaction on Wireless Communications.

[96] L. Wang, and Q. Liang, " UWB Sensor Networks in Hostile Environment: Interference Analysis and Performance Study," accepted by *IEEE Radio and Wireless Symposium 2007.*, Jan, 2007, Long Beach, CA.

[97] L. Wang, and Q. Liang, " UWB Sensor Networks in Hostile Environment: Interference Analysis and Performance Study," *Handbook of Wireless Mesh & Sensor Networking*, McGraw-Hill International, NY, 2006.

[98] W. Willinger, M. S. Taqqu, R. Sherman, and D. V. Wilson, "Self-similarity through high-variability: statistical analysis of ethernet LAN traffic at the source level," *IEEE Trans. on Networking*, vol. 5, no. 1, pp. 71-86, Feb 1997.

[99] M. Z. Win and R. A. Scholtz, "Ultra-wide Bandwidth Time-Hopping Spread-Spectrum Impulse Radio for Wireless Multiple Access Communications," *IEEE Transactions on Communications*, vol. 48, Issue: 4, pp. 679-691, April 2000.

[100] J. Winters, "On the capacity of radio communication systems with diversity in a Rayleigh fading environment," *IEEE J. Sel. Areas. Commun.*. vol. 5, pp. 871-878, June 1987.

[101] P. W. Wolniansky, G. J. Foschini, G. D. Golden, and R. A. Valenzuela, "V-BLAST: An architecture for realizing very high data rates over the rich-scattering wireless channel," *Proc. ISSSE*, Pisa, Italy, Sep. 1998, invited.

[102] Shibo Wu, and K. S. Candan, "GPER: Geographic power efficient routing in sensor networks," *Proceedings of the 12th IEEE International Conference on Network Protocols (ICNP'04)*, Berlin, Germany, Oct 2004.

[103] L. Yang and G. B. Giannakis, "A General Model and SINR Analysis of Low Duty-Cycle UWB Access Through Multipath With Narrowband Interference and Rake Reception," *IEEE Transactions on Communications*, Vol. 4, No. 4, pp. 1818-1833, July 2005.

[104] Y. Yao and G.B. Giannakis, "Energy-Efficient Scheduling for Wireless Sensor Networks," *IEEE Transactions on Communications*, vol. 53, Issure. 8, pp. 1333-1342, Aug 2005.

[105] O. Younis and S. Fahmy, "HEED: a hybrid, energy-efficient, distributed clustering approach for ad hoc sensor networks," *IEEE Transactions on Mobile Computing*, vol. 3, Issure. 4, pp. 366 - 379, Oct.-Dec. 2004

[106] L. A. Zadeh, " The concept of a linguistic variable and its application to approximate reasoning - I," *Information Sciences*, vol. 8, pp. 199-249, 1975.

BIOGRAPHICAL STATEMENT

Lingming Wang was born in Shanghai, China, in 1977. She received her B.S. degree from East China Normal University, China, in 1998, her M.S. degree from Shanghai Institute of Technical Physics, Chinese Academy of Sciences in 2001, both in Electrical Engineering. She is working toward the Ph.D degree in electrical engineering at University of Texas, Arlington, focusing on the physical layer of Wireless Sensor Networks, Ultra Wide Band communications.